UNIVERSITY OF BIRMINGHAM

School of Biosciences

Study of the Effects of Protein Corona on Nanoparticle-Membrane Interactions

A Research Project Submitted By

Abdullah Khan

As part of the requirement for the degree of MRes in Molecular Mechanistic Toxicology

This project was carried out at: The University of Birmingham, School of Biosciences, 8th Floor Laboratory

Under the supervision of: Dr Joshua Z. Rappoport

Date: August 2012

Table of Contents

I. Abstract Page

Within biological milieu, proteins adsorb onto the surface of nanoparticles to form a corona to drive the behaviour of nanomaterials *in vivo*. In a previous report, Smith *et al.* (2012) showed that the presence of serum inhibited interactions between carboxylate modified 20nm polystyrene nanoparticles and two cell lines (HeLa and MDCK), and caused a reduction in the surface charge of these nanoparticles. In this study the effects of different concentrations of serum and Bovine Serum Albumin (BSA) on the interactions between spherical carboxylated polystyrene particles and the plasma membrane are investigated. Similarly, the effects of varying concentrations of serum on the surface charge of these particles were also studied. 20nm, 200nm, and 1µm polystyrene particles were investigated, and it was found that the inhibitory effect of serum on nanoparticle-plasma membrane interactions was dependent on particle size and serum concentration. BSA was not found to induce the same level of inhibition at equivalent concentrations. The reduction in surface charge was shown to plateau at relatively low concentrations of serum (approximately 1%), suggesting that while the total amount of protein bound to these particles remained constant beyond this point, the composition of the corona would continue to change as serum concentration increased, thus causing increasing inhibition of particle-membrane interactions.

II. Acknowledgements

I would like to thank Dr Josh Rappoport for his patience and support throughout and beyond this project. Similarly I would like to thank Phil Smith, Dr Julie Mazzolini, and Jennifer Thorley for their supervision and guidance. The general support, advice, and kindness I received from the Rappoport research group and the rest of the 8th floor as a whole is very much appreciated.

I would also like to thank Dr Nik Hodges and Dr Anne Pheasant for their help throughout this course.

III. List of Figures Page

IV. List of Abbreviations

BSA: Bovine Serum Albumin

FBS: Foetal Bovine Serum

NP: Nanoparticle

DAPI: 4’,6-Diamidino-2-Phenylindole Dihydrochloride

SECTION 1: INTRODUCTION

Defined as materials with at least one dimension below 100nm, nanoparticles (NPs) exhibit a number of unique properties and behaviours that are proving invaluable in diverse medical and commercial roles (Zhang *et al.* 2011; McCall 2011; Weir *et al.* 2012). In this introductory section, the diverse applications of various nanomaterials are illustrated, as well as vehicular and industrial sources of particulate matter in the environment (Weir *et al.* 2012; Nohynek and Dufour 2012). The current concerns about the potentially harmful effects of nanoparticle exposure and usage will then be discussed in the context of the increasing exposure to nanoparticles as a consequence of their increasingly widespread use (Li *et al.* 2011; Libutti *et al.* 2010).

The behaviour of nanoparticles in physiological conditions will be explored, with a particular focus on the formation of a protein corona in biological media (Nel *et al.* 2009). Finally, previous work into the effects of the corona on nanoparticle interactions with cells will be presented as an introduction to the study reported here (Smith *et al.* 2012).

1.1 Commercial and Medical Applications of Nanoparticles

Silver and gold nanoparticles are classic examples of nanoparticles with broad commercial and medicinal applications (Dankovich and Gray 2011;Ghosh *et al.* 2008). Silver nanomaterials possess potent anti-microbial properties, and these have been exploited in a range of commercial fabrics and medical dressing materials (Maneerung *et al.* 2008; Zhang *et al.* 2009; Lorenz *et al* 2012). The anti-microbial properties of silver nanoparticles have

also been integrated into water filtration systems, both on their own and as part of nanocomposites, to provide a potentially effective, reliable, and cheap method of water purification which remains sorely needed in many parts of the world (Seo *et al.* 2012; Hillie and Hlophe 2007; Dankovich and Gray 2011).

Gold nanoparticles have proven effective in the field of cancer treatment, with applications in drug delivery and imaging (Llevot and Astruc 2012). The unique optical properties of gold nanoparticles allow for a novel method of imaging neoplasms through photoacoustic imaging, a technology which combines the high resolution offered by ultrasonic and the absorption contrast provided by optical imaging to offer a safe and effective method of imaging a wide range of pathologies (Li *et al* 2011).

As drug delivery vectors gold nanoparticles are rapidly emerging as effective and safe methods of delivering otherwise toxic therapies to malignancies (Figure 1) (Llevot and Astruc 2012). Aurimmune (CYT-6051), a therapy composed of 27nm gold nanoparticles functionalised with recombinant tumour necrosis factor alpha (rTNF-alpha) has successfully passed phase I trials, effectively delivering rTNF-alpha to tumours in human patients without demonstrating the severe hepatotoxicity and other side effects caused by the drug when delivered by other means (Libutti *et al.* 2010).

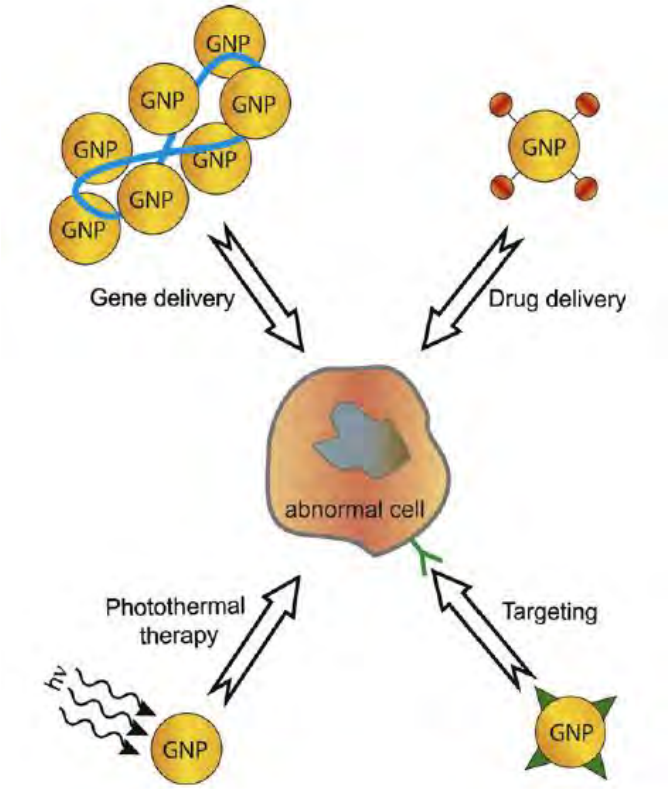

Figure 1 Image depicting the different therapeutic applications of gold nanoparticles (GNPs). These nanoparticles accumulate preferentially in tumours due to the Enhanced Permeability and Retention Effect (EPR), which is caused by the poor architecture and drainage typical of tumour vasculature. Because of EPR, gold nanoparticles passively target cancer cells and so are effective vectors for drug and gene therapies. Gold NPs can be further targeted by functionalization with tumour receptor specific ligands. GNPs can also be used for the thermal ablation of cancers, and these many uses of GNPs are being integrated into novel combinatorial approaches (Image from Ghosh *et al.* 2008).

A wide range of other materials have been used to generate nanoparticles with broad applications, including, carbon fullerenes and nanotubes which have found invaluable uses in fields as diverse as medicine, electrochemistry, and fuel cell technologies (Lota, Fic, and Frackowiak 2011; Yang *et al* 2012; Kosteralos, Bianco, and Prato 2009). Titanium oxide nanoparticles have found roles as important UV absorbers in skin products, photocatalysts, and next generation optical storage media (Yu, Ma, and Liu 2011; Ohkoshi *et al* 2010; Pinnell *et al.* 2000).

A number of personal care products contain nanoparticles, an example of these are sunscreens which contain NPs like titanium dioxide and zinc oxide (Nohynek and Dufour 2012). These nanoparticles are efficient absorbers of ultraviolet (UV) radiation and offer

significant benefits in terms of protecting skin cells from UV damage (Nohynek and Dufour 2012). Both zinc oxide and titanium dioxide are also used as additives in the food industry for their significant anti-microbial effects (Sharma, Anderson, and Dhawan 2012; Weir *et al.* 2012).

Despite the diverse uses for which nanoparticles are being developed, there remain a number of unanswered questions about their behaviour *in vivo*, particularly in terms of their potentially harmful effects (McCall 2011).

1.2 Concerns about Nanoparticle Safety

According to manufacturer reports there are an estimated 1,300 commercial products containing nanoparticles (McCall 2011). However there is currently no legislation in force that requires manufacturers to report on the presence of nanoparticles in their products, and as such the true number of products is likely to be much higher (Weir *et al.* 2012). What this means is that there is a potential for significant exposure to a variety of different nanoparticles which have yet to be identified and characterised in terms of their toxicity (harmful effects detrimental to cell or organ function and survival) (Weir *et al.* 2012; McCall 2011). This issue becomes particularly important as more and more nanoparticles are making their way into commercial usage, and hence general exposure (Weir *et al.* 2012; Nohynek and Dufour 2012).

Recent research has provided evidence of the toxic potential of zinc oxide particles, showing that exposure to these nanoparticles can result in toxic accumulation of reactive oxygen species (ROS) in human liver, bronchial, epithelial, and epidermal keratinocyte cell lines (Lee *et al.* 2012; Heng *et al.* 2010; Sharma *et al.* 2009; Sharma, Anderson, and Dhawan 2012). The accumulation of ROS, a cellular condition known as oxidative stress, can disrupt a number of important cellular processes and, if left unchecked, can cause DNA damage and ultimately cell death (Kirt and Appel 2004).

Oxidative stress has been observed as a consequence of exposure to titanium dioxide in human cell lines as well as *in vivo* systems like mice and Daphnia (Park *et al* 2008; Trouiller *et al.* 2009; Lovern and Klaper 2006). Titanium dioxide is a nanomaterial of

Figure 2 In a study of a range of popular commercially available food products substantial concentrations of titanium nanoparticles were found. Titanium nanoparticles can be detected in a number of different food products, and hence understanding the consequences of exposure to these particles is critical (Image from Weir *et al.* 2012).

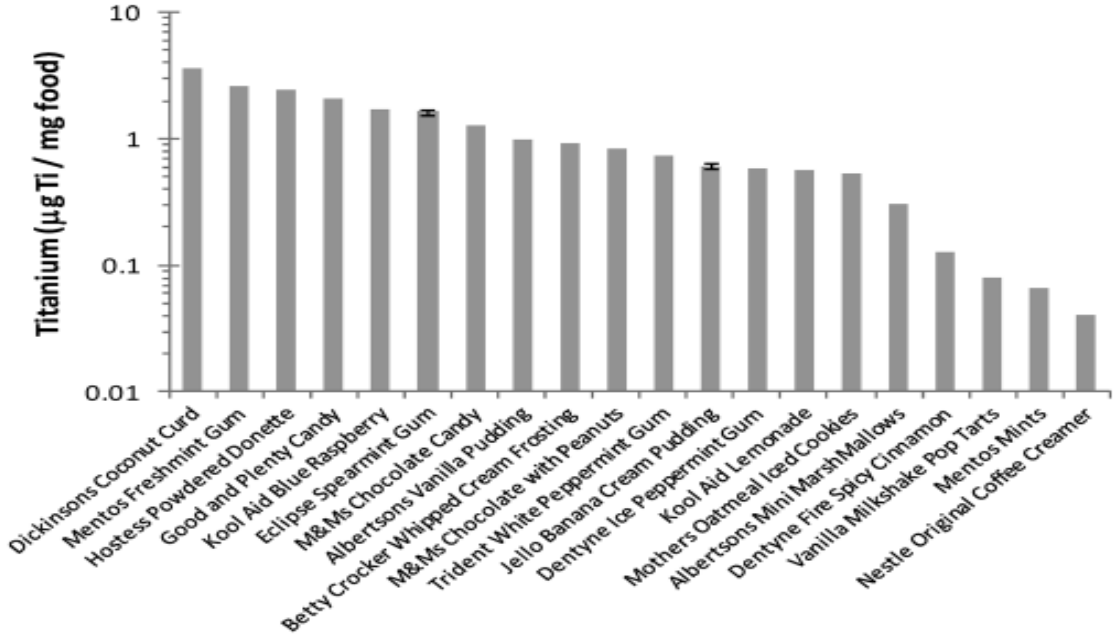

particular concern because of its widespread presence in commercial foods (Figures 2 and 3) (Weir *et al.* 2012).

However a criticism of these studies is that they do not effectively reproduce the conditions of exposure to these nanoparticles in the context of their use, and are not directly comparable to particles found in commercial products in terms of their physicochemical properties, surface functionalisation, and aggregation states (McCall 2011; Nohynek and Dufour 2012). As will be discussed in more detail in later Sections, these characteristics are critical to accurately evaluating the physiological effects of nanoparticles as they drive NP

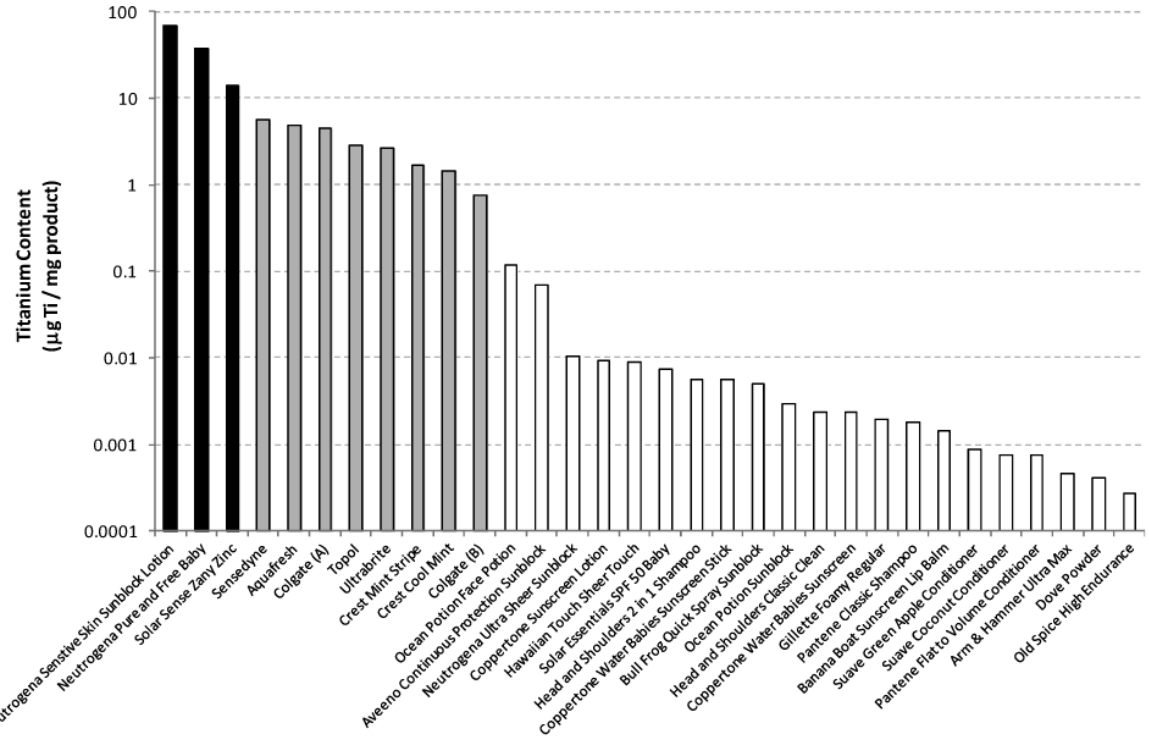

Figure 3 Graph depicting the concentration of titanium (present as titanium dioxide nanoparticles) found in a number of widely used commercial products. The presence of these nanoparticles in such a diverse range of products once again illustrates the need for an understanding of any potentially toxic effects of exposure to titanium dioxide (Image from Weir *et al.* 2012).

interactions with biological materials, and hence toxicity and pharmacokinetics (Jiang *et al.* 2008; Verma and Stellaci 2010; McCall 2011).

Concerns about potential toxic exposure have also been raised about a number of other nanomaterials making their way into use, the most notable being gold nanoparticles (Ghosh *et al.* 2008). The *in vivo* toxicity, distribution, absorption, and clearance of gold nanoparticles have only recently been characterised, and studies have shown that the toxicity of these particles is very much dependent on shape, surface chemistry, size, dose, and route of administration (Zhang *et al.* 2012; Goodman *et al.* 2004; Pan *et al.* 2007).

For example Zhang *et al.* (2010) have shown that orally and intraperitoneally administered 13.5nm citrate coated gold nanoparticles caused significant toxicity *in vivo* (evidenced by a reduction in blood cell count, spleen index, and body weight), while NPs of the same size and physicochemical properties administered intravenously by the same authors caused no discernible toxic effects. Cho *et al.* (2009) however, found that gold nanoparticles of the same size but different surface chemistry (the authors used gold NPs coated with polyethylene glycol (PEG)) caused acute liver toxicity after intravenous administration. Similarly toxicity through liver damage has been demonstrated in polyethylene glycol (PEG) functionalised gold nanoparticles of 10nm and 60nm diameters, while 5nm and 30nm particles did not demonstrate such an effect (Zhang *et al.* 2011).

Another example of nanoparticles making their way into medical application is that of iron oxides (Li and Chen 2011). These nanoparticles possess superparamagnetic properties

which make them invaluable imaging tools, particularly, for example, as contrast agents for the widely used magnetic resonance imaging (MRI) (Gupta *et al.* 2007). Iron oxide nanoparticles have passed through clinical trials as contrast agents for the MRI based detection of otherwise undetectable metastatic lymph node tumours (Harisinghani *et al.* 2003).

Studies into the toxicities of these nanoparticles remain relatively few in number, and while *in vivo* studies have generally shown that clinical doses of these nanoparticles are non-toxic, concerns have been raised about certain aspects of the distribution of these nanoparticles *in vivo* that have yet to be addressed (Li and Chen 2011; Kim *et al.* 2006). Toxicity through oxidative stress has been observed as a consequence of the exposure of iron oxide nanoparticles to lung cells, dermal cells (in conjunction with exposure to environmental levels of ultraviolet radiation) and neuronal cells, particularly in the hippocampal region of the brain (Murray *et al.* 2012; Kim *et al.* 2006; Ma *et al.* 2008; Zhu *et al.* 2008).

A number of investigations into the aforementioned effects of size, route of administration, and surface chemistry on the pharmacokinetics and toxicity of gold and iron oxide nanoparticles have been performed, however a discussion of these is beyond the scope of this introduction (Li and Chen 2011). It is important to note however, that as in the case of nanoparticles found in commercial products, there is a need for a more complete understanding of the toxicity of biomedical nanoparticles like gold and iron oxide (Li and Chen 2011).

In light of the expanding application of nanoparticles and the potential toxicities of a number of these nanoparticles highlighted by recent investigations, there is now an increasing awareness of the need for tighter safety legislation to regulate the production of nanoparticle based technologies based on an accurate understanding of nanoparticle interactions in biological systems and their toxicities (McCall 2011; Weir *et al.* 2011). These safety concerns are not limited to nanoparticles found in commercial and medical products however, and extend to NPs generated by industrial and vehicular processes.

1.3 Nanoparticles and Environmental Exposure

Investigations into the production of nanoparticles as a byproduct of vehicle exhaust and a number of manufacturing processes have revealed that these sources generate a number of potentially toxic particles with serious environmental health consequences (Canagaratna *et al.* 2010; Wang *et al.* 2011).

Emissions from both diesel and gasoline based vehicles are now known to be rich in nanoparticles (Sakurai *et al.* 2003; Tobias *et al.* 2001). Analysis of the nanoparticles found in these emissions has shown that they are largely highly volatile organic particles around 50nm in size formed from unburned fuel and lubricating oil, as well as a small number of sulfuric acid nanoparticles (Fushimi *et al.* 2011; Sakurai *et al.* 2003; Tobias *et al.* 2001).

Similarly a number of widely used manufacturing processes like heat treatment, threading, high speed machining, and welding have been shown to generate nanoparticles (Heitbrink *et al.* 2007; Thornburg *et al.* 2000; Wang *et al.* 2011). These processes make use of semi-

volatile mineral oil-based metalworking fluids (MWFs) which are thought to form nanoparticles as a consequence of the heating of these fluids in manufacturing settings (Thornburg and Leith 2000).

Nanoparticles generated by vehicles and industrial processes contribute significantly to the increasing presence of ambient particulate matter (PM) in the environment, a factor which has been shown to pose a significant toxicological concern particularly due to exposure to the respiratory tract (Figure 4) (Li, Xia, and Nel 2008). Exposure to PM has been identified as a causative factor in incidences of cardiovascular and pulmonary disease, and thus far oxidative stress is thought to be the major mechanism by which nanoparticles in the environment cause disease and mortality (Grahame and Schlesinger 2012; Ayres *et al.* 2008; Li, Xia, and Nel 2008).

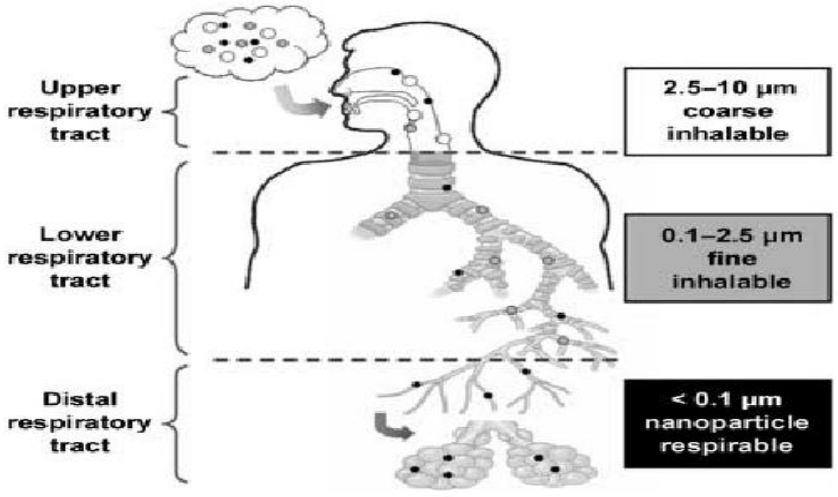

Figure 4 Ambient particulate matter, a by-product of industrial and vehicle processes, includes a diverse range of particles of different sizes, shapes, and compositions. Amongst these are nanoparticles, which distribute to alveoli and elements of the distal respiratory system and can cause incidences of serious pulmonary disease. (BeruBe *et al.* 2007).

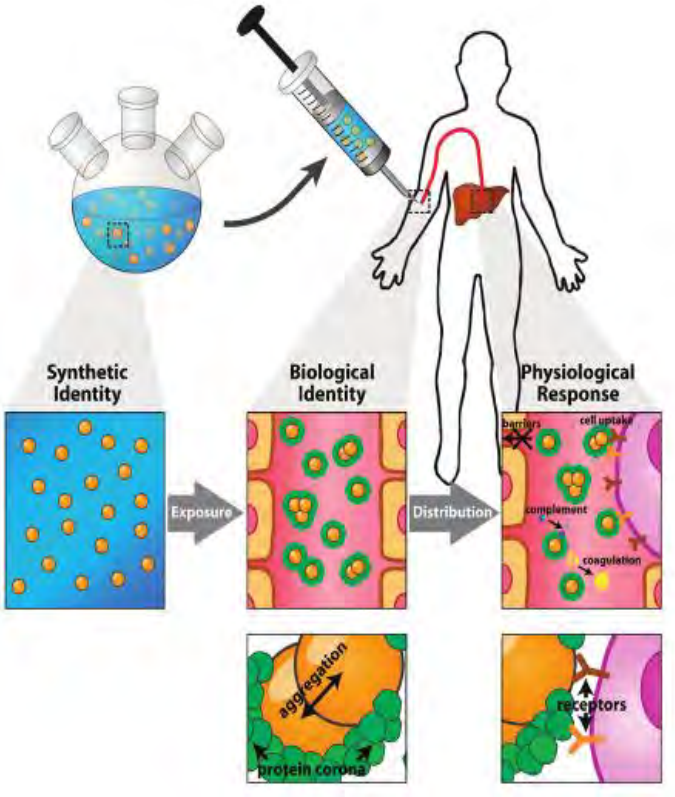

Figure 5 Figure illustrating the distinction between the synthetic identity of nanomaterials and the biological identity assumed once within biological media. While the many physical and chemical properties of nanoparticles drive adsorption events which form distinctive protein coronas, it is the corona and the unique biological identity it confers to nanomaterials in biological environments that affects interactions with cells both *in vitro* and *in vivo*. The corona is key to the physiological response to nanoparticles, and can affect absorption, distribution, and clearance (Image from Walkey and Chan 2011).

1.4 Nanoparticles in Physiological Environments and the Protein Corona

Upon exposure to physiological environments, nanoparticles develop a distinct biological identity which dictates their behaviour within that particular milieu (Figure 5) (Walkey and Chan 2011; Nel *et al.* 2009). This biological identity involves the formation of a protein corona around nanoparticles exposed to specific media such as serum or plasma (Nel *et al.* 2009).

This corona has been shown to dictate diverse elements of the *in vivo* and *in vitro* response to nanoparticles, including uptake, plasma membrane binding, transport, aggregation, and toxicity (Walkey and Chan 2011; Nel *et al.* 2009). Therefore an understanding of the formation of the protein corona and its consequent effects is absolutely critical to

$$\Delta G_{\text{ads}} = \Delta H_{\text{ads}} - T\Delta S_{\text{ads}} < 0,$$

Figure 6 Equation describing the binding energy of adsorption events. Here ΔG_{ads} is the change in Gibbs Free Energy (the binding energy of an adsorption event), ΔH_{ads} is the change in enthalpy during adsorption, T is temperature, and ΔS_{ads} is the change in entropy that occurs during adsorption (Walkey and Chan 2011).

effectively developing nano-therapies with controlled physiological absorption and distribution kinetics, as well as understanding the toxicity of nanoparticles present in the environment (Sanfins *et al.* 2011).

1.4.1 Mechanisms and Kinetics of Corona Formation

The current understanding of the mechanisms and kinetics of corona formation is that the binding energies of adsorption events (Figure 6), and hence their thermodynamic favourability, is dependent on protein structure and the physicochemical properties of the nanoparticles themselves (De *et al.* 2007).

Energetically favourable changes include covalent and non-covalent bonding, as well as conformational changes (in either protein structure or the surface of the nanoparticles in question) (Walkey and Chan 2007).

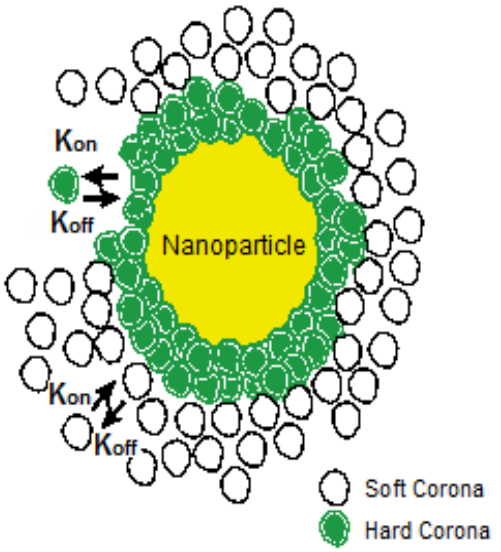

Figure 7 In this figure the formation of a distinctive protein corona around nanoparticles is modeled in terms of adsorption and desorption constants. The corona is currently thought to be comprised of two distinct elements in terms of adsorption/desorption rates and binding energies, and these are the soft and hard corona. The hard corona is typified by high binding energy adsorption events of high affinity proteins that associate closely with the surface of nanomaterials, while the soft corona is thought to be comprised of lower affinity proteins which adsorb via protein-protein interactions. K_{on} is the association constant, while K_{off} is the dissociation constant. K_{on} is dependent on both the binding affinity of a protein (and hence the likelihood of a binding event) and the concentration of said protein. K_{off} is based on the binding energy of the adsorption events (Image adapted from Walkey and Chan 2011).

The stability of protein-nanoparticle binding is dependent on the binding energy of the adsorption event involved (Walkey and Chan 2007; Casals *et al.* 2010). Generally, proteins with large binding energies remain associated with nanoparticles over longer periods of time, and form what is referred to as the 'hard corona', while proteins that adsorb with low binding energies form a 'soft corona' which is easily desorbed back into solution (Figure 7) (Casals *et al.* 2010).

The binding energy of each adsorption event is determined by the structural composition of proteins and the physicochemical properties of the nanoparticles with which they are interacting (De *et al.* 2007). For instance, nanoparticles with charged surfaces are likely to form stable bonds with hydrophilic proteins (De *et al.* 2007).

The induction of conformational changes during corona formation has important consequences on interactions between nanoparticles possessed of a corona and their physiological environment (Shang *et al.* 2007; Mahmoudi *et al.* 2011). These rearrangements can expose domains and sequences that would not otherwise be available for interactions, and as such can have significant consequences on the pharmacokinetics of nanoparticles *in vivo* (Shang *et al.* 2007). Moreover these newly bared moieties can result in protein-protein interactions which may further alter the composition of the protein corona (Mahmoudi *et al.* 2011).

In a study into the kinetics of corona formation, Cedervall *et al.* (2007) generated a model in which proteins were divided into groups according to their rates of association and dissociation to the copolymer nanoparticles used by the authors (Figure 7).

The first group was characterised by rapid adsorption (within seconds) associated with the formation of a stable hard corona, which was also shown to demonstrate slow desorption (over a period of hours) (Cedervall *et al.* 2007). Conversely the second group demonstrated a slow rate of association and rapid dissociation reflective of the low affinity binding of the soft corona (Cedervall *et al.* 2007).

Protein adsorption, and hence corona formation, is a highly dynamic process in the context of nanoparticles in physiological environments (Casals *et al.* 2010; Sanfins *et al.* 2011). The association and dissociation of various proteins over time is referred to as the Vroman

Effect, which states that the composition of the corona can change over time while the total protein content remains relatively unchanged (Sanfins *et al.* 2011; Casals *et al.* 2010).

Interestingly in the context of physiological media the abundance of proteins strongly affects initial binding events, and it has been shown that the early stages of the Vroman Effect in plasma will involve the rapid binding of low affinity but highly abundant proteins like albumin and Immunoglobulin G (Dell'Orco *et al.* 2010). These are rapidly displaced by high affinity molecules like apolipoproteins within seconds (Dell'Orco *et al.* 2010; Casals *et al.* 2010). This illustrates the complexity of the kinetics of protein corona formation, which is dictated by a number of factors that are closely interlinked.

Protein binding to nanoparticles can result in a conformational change provided that such a change would allow for an energetically favourable interaction between either charged or hydrophobic regions of the nanoparticles and the proteins in question (Gessner *et al.* 2000). Whether such conformational changes are induced during adsorption also depends on other physicochemical properties of both nanoparticles and proteins involved, for example proteins with disulfide bonds or other strong internal bonds are less likely to undergo a conformational change (Walkey and Chan 2011).

1.4.2 Composition of the Corona

Investigations into the composition of the protein corona to date show that the protein corona is complex and highly individual to the nanomaterials in question and the media in which they are found (Walkey and Chan 2011). Analyses of protein coronas on a number of

different nanoparticles have revealed that approximately 125 different proteins with varying physiological roles can adsorb onto the surface of various nanomaterials and form part of a unique and distinctive protein corona.

The physicochemical composition and surface chemistry of nanoparticles have been shown to be major determining factors in the formation of a distinct protein corona, and hence the fate of nanoparticles both *in vivo* and *in vitro* (Walkey *et al.* 2011; Sanfins *et al.* 2011; Nel *et al.* 2009). Other characteristics of nanoparticles that dictate their interactions with biological materials include shape, hydrophobicity or hydrophilicity, surface architecture (crystallinity or heterogeneity), aggregation, and zeta potential (Verma and Stellaci 2010; Patil et al 2007).

The role these properties have to play in corona formation is demonstrated by a body of proteomic studies which illustrate the depth and diversity of proteins involved in corona formation (Figure 8), and how the properties of various nanomaterials influence the composition of the corona (Lundqvist *et al.* 2008; Deng *et al.* 2009). In an analysis of the corona formed on 50nm and 100nm polystyrene nanoparticles with different surface charges (positive, negative, and uncharged), Lundqvist *et al.* (2008) found that both size and charge influence which proteins bind to form the corona.

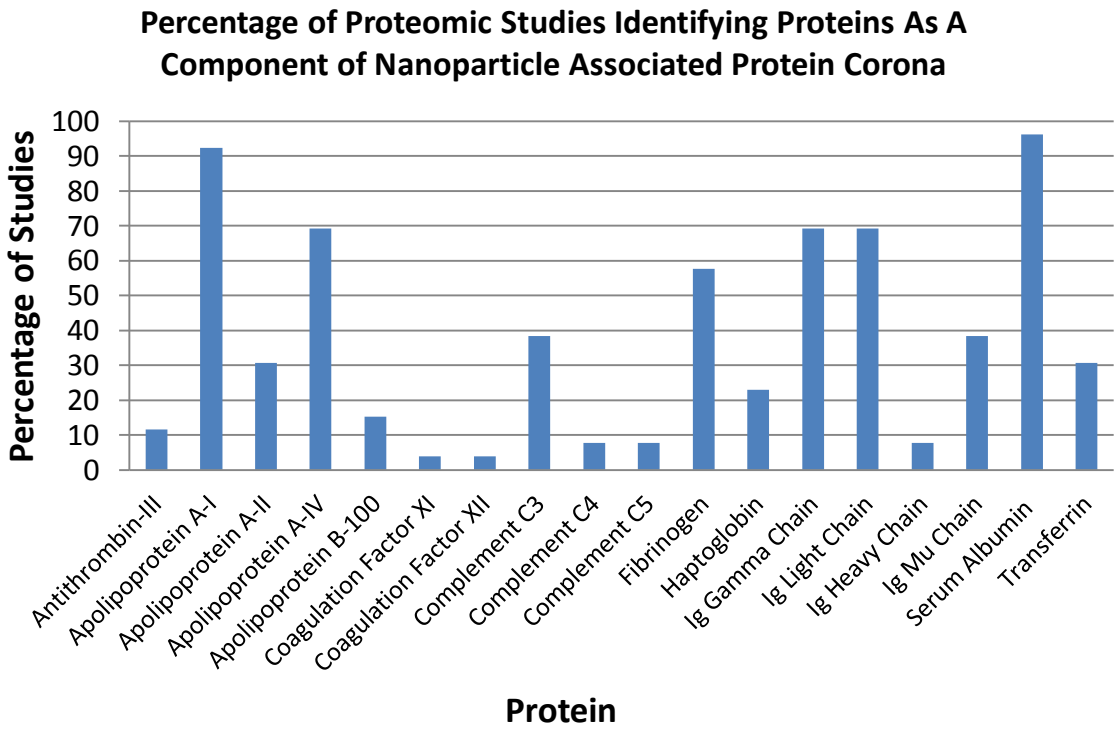

Figure 8 In a review of the literature to date, Walkey and Chan (2011) compiled an adsorbosome of 125 proteins reported as elements of the protein corona in 26 separate studies into corona composition. In this figure the detection of key proteins of interest are represented in terms of the percentage of studies in which they are observed. Interestingly Apolipoprotein A-1, despite its relatively low abundance when compared to other plasma proteins, is detected in approximately 90% of the 26 studies reviewed. While Ig Gamma and Light Chains are observed across a range of nanomaterials, the Heavy Chain Immunogobulin is detected in a relatively small number of such studies (Adapted from Walkey and Chan 2011).

For example, the authors found that apolipoproteins were a major part of the corona formed on positively charged (amine modified nanoparticles), whereas these lipoproteins were barely present on negatively charged (carboxylate modified) NPs (Lunqvist *et al.* 2008). In some cases these differences were remarkably specific, as demonstrated by apolipoprotein B-100 which did not bind to 50nm particles regardless of surface chemistry, and yet was

found in abundance on 100nm NPs of all three surface charges tested (positive, negative, and neutral) (Lundqvist *et al.* 2008).

In a comparison of three metal oxide nanoparticles (titanium dioxide, zinc oxide, and silicon dioxide) with the same surface charge Deng *et al.* (2009) showed that these factors strongly affected which proteins bound these nanoparticles, and hence the composition of the corona. The authors found that while very similar proteins contributed to the corona of titanium and silicon dioxide particles, zinc oxide nanoparticles adsorbed markedly different proteins (Deng *et al.* 2009).

The authors found that certain proteins (e.g. Clusterin, Apolipoprotein D, and Alpha-2-acid glycoprotein) would adsorb to titanium and silicon dioxide particles and yet were not detected on zinc oxide (Deng *et al.* 2009). Interestingly the reverse was also true, and proteins like Transferrin, Ig Heavy Chain Alpha, and Haptoglobin (alpha) were found bound to zinc oxide nanoparticles alone (Deng *et al.* 2009).

Deng *et al.* (2009) also investigated the impact of shape on protein binding to titanium dioxide nanoparticles, and found a similar pattern of exclusivity in certain cases. Clusterin and Apolipoprotein D for example would only bind to spherical nanoparticles, and were not found associated with nanorods or –tubes (Deng *et al.* 2009).

These examples should illustrate the fact that the composition of the protein corona varies in response to a number of different nanoparticle properties (Deng *et al.* 2009; Lundqvist *et al.* 2008). However as more investigations into corona composition are performed some

patterns of adsorption are emerging. The binding of apolipoproteins for example, has been shown to be an essential part of the formation of a stable hard corona on hydrophobic nanoparticles (as a consequence of interactions between hydrophobic surfaces and the lipid binding domain possessed by apolipoproteins) (Gesner *et al.* 2000; Cedervall *et al.* 2007). On the other hand, IgG, Fibrinogen, and Albumin typically adsorb on to the surfaces of hydrophilic nanoparticles preferentially (Gesner *et al.* 2000; Cedervall *et al.* 2007).

Beyond the properties of NPs themselves, the composition of the biological media in which they are found is key in determining the formation of a protein corona, and subsequently the interactions between those nanoparticles, now possessed of a distinct biological identity, and cellular materials (Nel *et al.* 2009). This is an area which has yet to be thoroughly investigated, and is an important aspect of the study reported here.

1.5 Previous Work and Aims of Study

Previous work in this lab conducted by Smith *et al.* (2012) revealed a serum-sensitive pathway of carboxylate modified polystyrene nanoparticle binding and uptake to and into HeLa cells. The authors found that when comparing nanoparticle interactions with cells in serum free and 10% serum containing media, twenty-fold inhibition was observed in the latter across a number of different time courses (Figure 9) (Smith *et al.* 2012). Furthermore, a three-fold reduction in zeta potential was observed when comparing serum free (approximately -32mV) and serum containing media (approximately -10mV) (Smith *et al.* 2012).

These findings suggested that the inhibitory effect of serum on the binding and uptake of polystyrene nanoparticles by HeLa cells could potentially be a consequence of a reduction in surface charge caused by the formation of a protein corona (Smith *et al.* 2012). Therefore with these findings in mind, this study aims to further investigate the relationship between serum, surface charge (measured by zeta potential), and nanoparticle interactions with the plasma membrane.

The importance of surface charge as a factor influencing nanoparticle interactions with

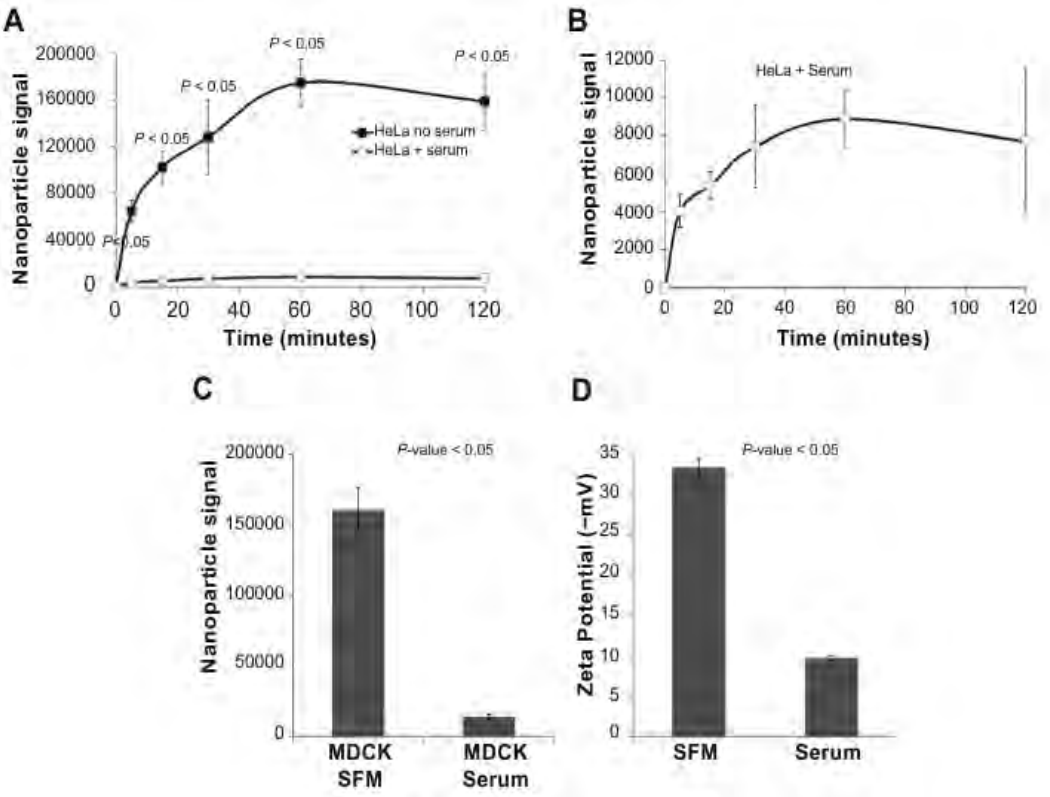

Figure 9 Image demonstrating differences in zeta potential and cell-associated nanoparticle signal in serum containing and serum free media. A and B) Cell-associated nanoparticle fluorescence measured over a 120 minute time course. A twenty-fold reduction in signal was observed, and was reproduced in C) MDCK cells. D) Three-fold reduction in zeta potential due to the presence of serum (Smith *et al.* 2011).

biological media has been well established, and as such this study investigated particles with the same surface carboxylate modification as Smith *et al.* (2012) to allow for an accurate and comparable investigation into the effects of different serum concentrations (Nel *et al.* 2009). Size is another variable that has been shown to strongly affect nanoparticle behaviour, and while particles of the same diameter as those previously reported by Smith *et al.* (2012) were investigated (20nm), 200nm and 1µm carboxylate modified polystyrene particles were also investigated to explore the effects of size on the serum induced reduction of particle-cell interactions and surface charge. (Jiang *et al.* 2008; Walkey *et al.* 2012)

Furthermore, Bovine Serum Albumin (BSA), the most abundant protein in serum and plasma, was investigated to ascertain whether or not this protein could induce similar effects on membrane-nanoparticle interactions and zeta potential (Chakraborty *et al.* 2011).

SECTION 2: MATERIALS AND METHODS

2.1 Cell Culture

The experiments reported in this study were performed on HeLa cells (Health Protection Agency Culture Collections, Salisbury, United Kingdom) incubated with 5% carbon dioxide at 37°C. Cells were grown in 75cm^2 cell culture flasks (Contig) with serum containing media composed of 10% Foetal Bovine Serum (BioSera), 1% penicillin and streptomycin (Invitrogen), and Dulbecco's Modified Eagle Medium (DMEM) (Lonza).

For passaging and plating for the experiments described herein cells were first detached by incubation with trypsin (Invitrogen) for 5 minutes at 37°C, then re-suspended in serum containing media described above. This suspension was then placed into new flasks and diluted appropriately, or onto the plates relevant to the experiment to be performed (96 well plates for plate reader experiments (Section 2.3) and onto 22mm coverslips housed on six-well plates for wash experiments (Section 2.5)).

2.2 Nanoparticles Used

The nanoparticles used in this study were carboxylate modified fluorescent yellow/green polystyrene FluoSpheres (Invitrogen). Particles at 20nm, 200nm, and 1µm diameters were used, and these were provided in suspensions at 2% solids with water and 2mM sodium azide.

$$\text{Number of microspheres/ mL} = \frac{6C \times 10^{12}}{\rho \times \pi \times \phi^3}$$

Where: C = concentration of suspended beads in g/mL
(0.02 g/mL for a 2% suspension)
ϕ = diameter of microspheres in µm
ρ = density of polymer in g/mL (1.05 for polystyrene)

Figure 10 Formula for the deduction of the total number of FluoSpheres present in a given volume of suspension provided by Invitrogen and used to determine the concentrations of 20nm, 200nm, and 1µm particles at which total surface area would be constant (Image from Invitrogen).

The concentration of nanoparticles of these sizes used in this study was scaled (taking account the number of particles in suspension) so that the same total surface area was available for adsorption, thereby allowing for comparability between studies performed on particles of different sizes. Using the formula provided by Invitrogen (Figure 10), it was determined that to match the total surface area of 20nm particles in 2% suspensions at a 1:1000 dilution, a 1:100 dilution of 200nm particles and a 1:200 dilution of 1µm particles would be needed.

2.3 Plate Reader Experiments

To determine nanoparticle binding to the plasma membrane, carboxylated polystyrene FluoSpheres of varying diameters were incubated with HeLa cells for 15 minutes with varying concentrations of either Foetal Bovine Serum (FBS) or Bovine Serum Albumin (BSA) (Sigma). 0%, 0.05%, 0.25%, 1%, 2.5%, 5%, and 10% concentrations of FBS were used and each concentration tested in triplicate three times (n = 3. Equivalent concentrations of BSA were used made from a stock solution of BSA at a concentration of

15.4 g/l, the amount of BSA reported by BioSera to be present in FBS. This allowed for comparable data points at which the amounts of BSA present were equivalent to those in FBS. The polystyrene FluoSpheres used were incubated with HeLa cells for 15 minutes, as it this point these particles are largely bound to the plasma membrane as illustrated by Figure 11, therefore allowing the plate reader data to be interpreted as a measure of nanoparticle binding to the cell surface.

Cells were detached with trypsin as per the method described in Section 2.1 prior to plating in uClear black 96-well glass bottomed plates (Greiner Bio) and incubation for approximately 24 hours at 37°C in the presence of 5% carbon dioxide. Cells were then serum starved for 15 minutes in DMEM, before being treated with 100µl of the relevant concentrations of either BSA or FBS and FluoSpheres at diameters of either 20nm, 200nm,

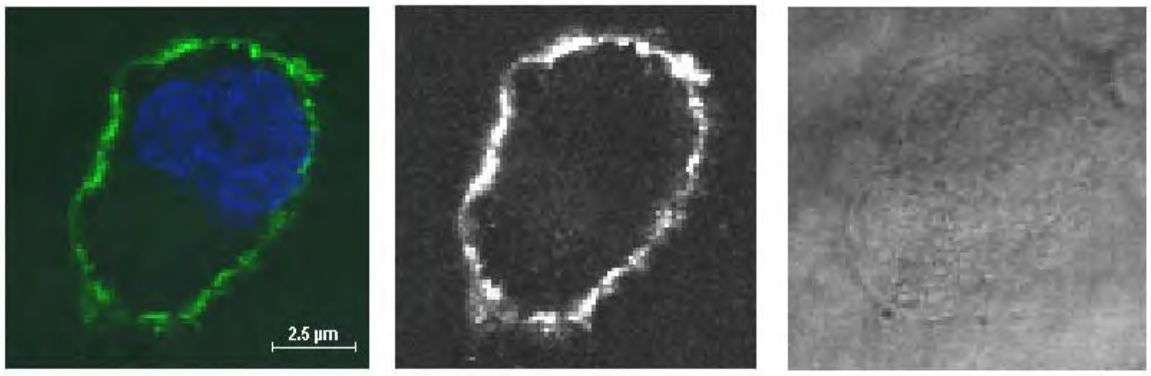

Figure 11 Confocal microscope images illustrating the binding of 20nm carboxylate modified yellow/green polystyrene nanoparticles to the plasma membrane of a HeLa after a 15 minute incubation. This point in time was chosen as the focus of the plate reader study so that the signal detected by the plate reader could be accurately interpreted as membrane associated. A) Shows both yellow/green polystyrene nanospheres and DAPI nuclear staining. B) An image using the green laser of an inverted A1R Nikon Confocal Microscope scaled for brightness placed next to C) a transmitted light image to show that nanoparticles are in fact binding to the plasma membrane.

or 1µm and incubated for a further 15 minutes at 37°C.

After this incubation the treatment solution was removed and cells were washed twice with 100µl of phosphate buffered saline (PBS) (Lonza) before fixing with 100µl of 4% paraformaldehyde (PFA) for 5 minutes at room temperature (Electron Microscopy Sciences). Post-fixation the PFA solution was removed and cells rinsed a further two times with 100µl PBS. Analysis of these treated samples was then performed with cells in 100µl PBS using a FLUOStar Omega Fluorescence Plate Reader (BMG LABTECH GmbH).

2.4 Zeta Potential Measurements

Zeta potentials of 20nm, 200nm, and 1µm Carboxylated FluoSpheres in different concentrations of FBS and BSA were determined using the Malvern Zetasizer Nano ZS ZEN3600 (Malvern Instruments). 2ml samples of 20nm, 200nm, and 1µm FluoSpheres were prepared at the aforementioned concentrations (Section 2.2) in 0%, 0.025%, 0.05%, 1%, and 10% concentrations of FBS and 15/4 g/l BSA stock solution.

2.5 Development of Protocol to Remove Membrane Bound Nanoparticles

As a part of this project an attempt was made to establish a protocol to remove membrane bound nanoparticles and allow for the study of nanoparticle internalisation by means of a plate reader assay as described in Section 2.3.

To this end cells were plated in 6-well plates on 22mm glass coverslips for approximately 24 hours before 15 minutes of serum starvation in 2ml DMEM followed by a 15 minute

incubation with 20nm nanoparticles in serum free DMEM at a dilution of 1:1000. The cells were then rinsed twice with 2ml of PBS prior to 5 minutes fixation in 1ml of 4% PFA. coverslip were then mounted on glass slides with Vectashield (Vector Laboratories Ltd) for imaging with the 60x oil objective of a Nikon A1R Inverted Confocal Microscope (Nikon Corporation).

To ensure that images were taken and compared on the same focal plane, slides were captured as Z-stacks and the image possessing the broadest DAPI nuclear stains selected as the mid-section of the cell.

After treatment with the nanoparticle solution a number of different wash protocols were tried. These included 10 second, 30 second, 60 second, and 90 second trypsin (Invitrogen) and Accutase (Invitrogen) washes, as well as a series of Hank's Balanced Salt Solution (HBSS) washes which had been shown by other authors to remove membrane bound nanoparticles (Georgieva *et al.* 2010; Rejman *et al.* 2004).

SECTION 3: RESULTS

3.1 FluoSphere Binding to the Plasma Membrane in Varying Concentrations of Serum as Determined by Plate Reader

The plate reader data from the serum experiments described in Section 2.3 are presented in Figure 12. The plate reader data has been normalised to 1 to better represent the exponential decay of membrane associated fluorescent signal as a result of increasing serum concentration.

The data indicates that the inhibitory effect of serum on the binding of carboxylate modified polystyrene FluoSpheres is size dependent, with the reduction of membrane associated signal at 10% serum 10-fold less for 1µm particles than 20nm nanoparticles, and 3-fold less for 200nm FluoSpheres when compared to their 20nm counterparts.

Statistical testing in this study was performed using the Student's t-test, which allowed for a comparison of the raw data between 20nm and 200nm particles and 200nm and 1µm particles. This method allows for an accurate comparison between data sets based on the actual data reported (Rice 1989).

The t-tests comparing 20nm nanoparticles to 200nm and 1µm particles found that while the 1µm data was significantly different to the 20nm data, only 3 data points at 200nm (at 10%, 2.5%, and 1% serum) were statistically different (Figure 12) when compared to 20nm.

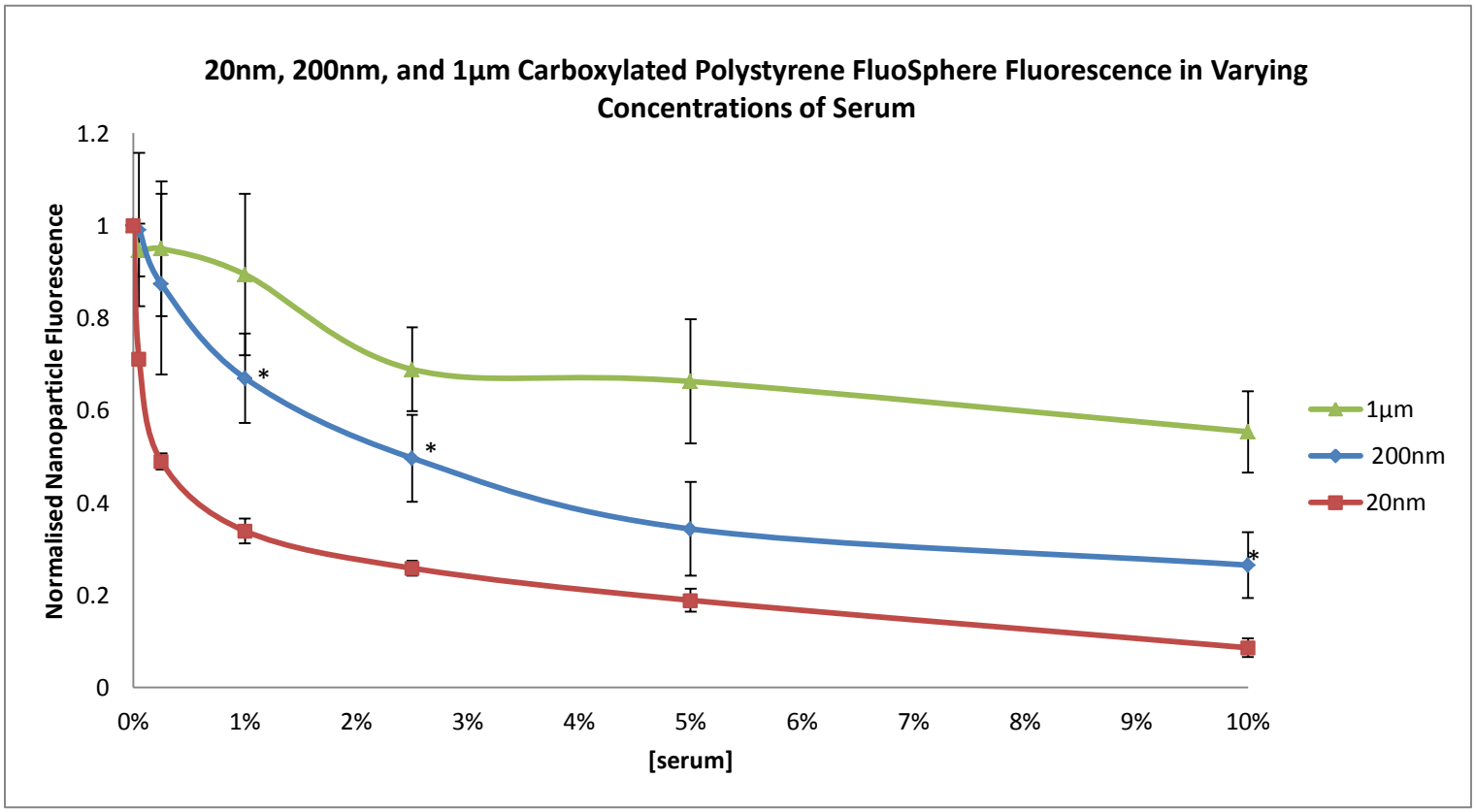

Figure 12 Line graph demonstrating the inhibitory effect of different concentrations of serum on carboxylate modified yellow/green polystyrene FluoSphere (20nm, 200nm, and 1µm diameters) binding to the plasma membrane after 15 minute incubations. The graph shows that the inhibitory effect of serum on nanoparticle fluorescence (a measure of membrane binding after 15 minutes of incubation) is size dependent, and is dramatically reduced at 1µm when compared to 200nm and 20nm. A Student's t-test revealed that all 1µm data points presented here were statistically significant (p-value < 0.05) when tested against the 20nm data, while only three 200nm data points (indicated by asterisks) were significantly different (p-value < 0.05) when compared to 20nm data. (Error bars indicate standard error of the mean).

3.2 Polystyrene FluoSphere Zeta Potentials in Serum

While the plate reader showed an exponential decline in membrane-associated FluoSphere signal, the zeta potential data illustrated by Figure 13 shows a rapid decrease in zeta potential at the lowest concentrations of serum (0.025%) for all three sizes of polystyrene FluoSpheres studied. The reduction in zeta potential plateaus sharply between 0.05% and 1% and the total 3-fold reduction in zeta potential is achieved at approximately 1%, whereas membrane binding as demonstrated by the plate reader data in Figure 11 of particles of all three sizes continues to decline and does not reach a saturation point even at 10%.

Figure 13A represents the raw zeta potential data and there is an observable and statistically significant difference between each data set. The instrument measures zeta potentials via electrophoretic motility, and so as the trends evidenced by each data set are similar the differences in zeta potential magnitude can potentially be attributed to the fact that differently sized particles will have different motilities in suspension (O'Brien, Cannon, and Rowland 1995).

To determine whether or not the differences observed between each data set were due to size-dependent variations in motility, and hence zeta potential measurement, a second graph (Figure 13B) is included in which the data illustrated in Figure 12A has been normalised to 1. Interestingly t-testing the normalised data showed that the only the 0.025% and 0.05% data points of 1μm and 200nm measurements were statistically significantly different to their 20nm equivalents.

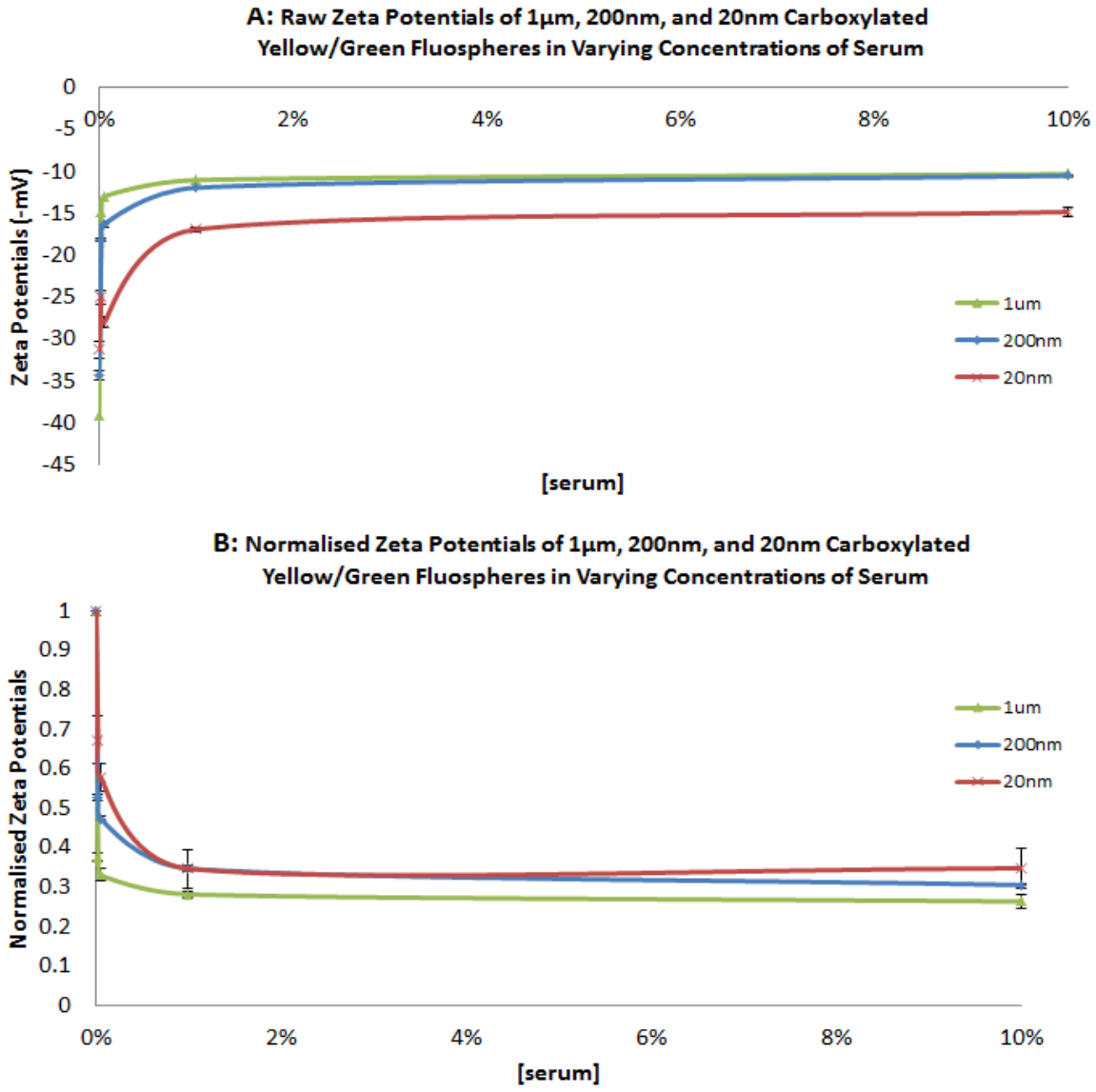

Figure 13 A) Graph illustrating the raw zeta potentials of 20nm, 200nm, and 1µm carboxylate modified yellow/green polystyrene FluoSpheres in varying concentrations of serum. The introduction of even small concentrations of serum results in a sharp decrease in the measured zeta potentials of particles of all three sizes. All differences between 20nm and 1µm and 20 nm and 200nm FluoSpheres were shown to be statistically significant by a Student's t-test. While this trend is comparable across all three data sets, the magnitude of the zeta potentials recorded varies by particle size, which may be attributable to the effect of size on electrophoretic motility (from which zeta potential is calculated). B) Normalised zeta potential data plotted to demonstrate the similarity in trends between the differently sized FluoSpheres tested. Here differences between 20nm and 1µm and 20nm and 200nm particles at 0.025% and 0.05% were statistically significant (p-values < 0.05). (Error bars indicate standard error of the mean).

3.3. Plate Reader Bovine Serum Albumin (BSA) Data

As shown by Figure 14, BSA does not inhibit the binding of polystyrene FluoSpheres to the plasma membrane to the same extent as serum. 20nm carboxylate modified particles only demonstrated a 4-fold reduction in binding, while 200nm and 1µm showed an approximately 1.6-fold inhibition (Figure 14). This is also illustrated by Figure 15 which directly compares 20nm nanoparticles in serum and BSA and clearly illustrates the substantial difference between the two data sets.

Figure 14 Graph demonstrating the effect of different concentrations of BSA, prepared in quantities equivalent to those found in similar concentrations of serum, on the membrane binding of 20nm, 200nm, and 1µm carboxylate modified polystyrene FluoSpheres. Between 0% and 10% there is a size dependent reduction in the observed membrane associated nanoparticle fluorescence, however at lower concentrations there is a reproducible, if not statistically significant, increase in membrane binding. In a comparison between 20nm data and 200nm and 1µm using the Student's t-test, only data at 1% and 10% BSA were found to be statistically significant (p-values < 0.05).

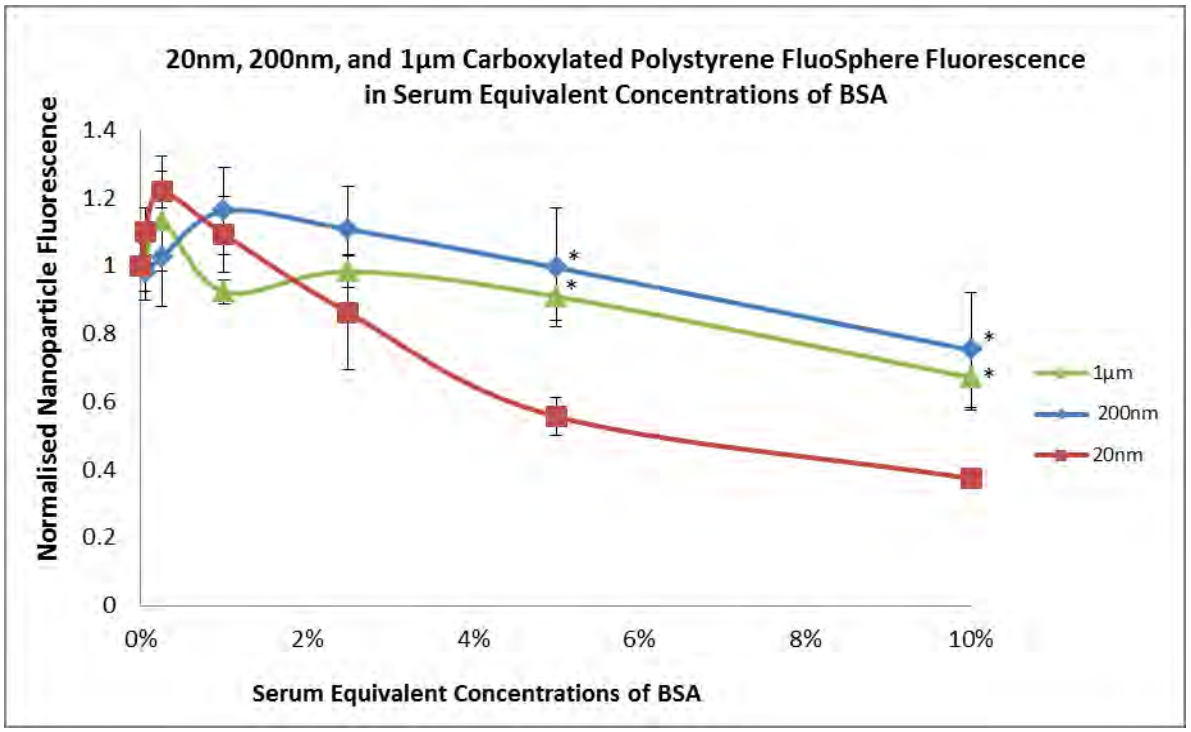

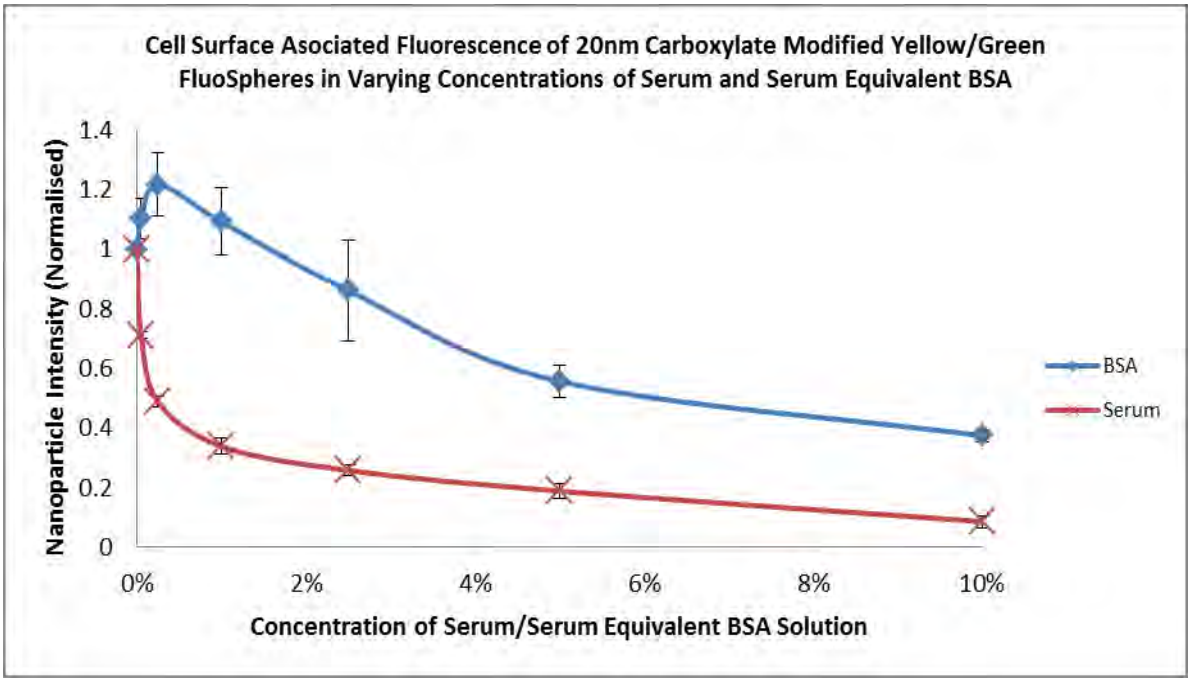

Figure 15 Graph comparing the reduction in plasma membrane associated fluorescence of 20nm carboxylate modified yellow/green polystyrene nanoparticles in the presence of different concentrations of serum and bovine serum albumin (BSA) at 15.4 g/l, a concentration equivalent to the amount of the protein found in serum. The graph shows that while BSA causes a reduction in the plasma membrane associated nanoparticle associated fluorescence, it is not equivalent to the serum effect. At low concentrations of BSA 20nm polystyrene nanoparticles exhibit an increase in plasma membrane binding which is not statistically significant when compared to the signal at 0% BSA ($p < 0.05\%$) after t-testing. (Error bars indicate standard error of the mean).

Interestingly an increase in FluoSphere binding was observed at low concentrations of BSA. However this increase, while reproducible and evident in each of the three sizes tested, was not statistically significant when compared to values at 0% using a Student's t-test. Furthermore when comparing the 20nm to 200nm and 1µm data using the same test statistically significant differences were observed only at 1% and 10% BSA.

3.4 Zeta Potentials in BSA

As shown in Figure 16, there is an exponential reduction in zeta potential (ZP) caused by the presence of BSA. As in the case of the serum data (Figure 12), the change in zeta

potential is not size dependent and when normalised (Figure 16B), and only one data point (0.05%) is significantly different (p-value < 0.05) when 200nm and 1µm particles are compared to 20nm data using a Student's t-test.

However when compared to the zeta potentials measured in serum, the magnitude of this change and the rate at which it occurs is markedly different. Where a 3-fold change in zeta potentials was observed between 0% and 10% serum, 10% BSA at a concentration equivalent to the quantities of the protein found in serum (15.4g/l) only induced a 2-fold reduction in ZP (illustrated in the case of 20nm particles by Figure 17).

The 20nm zeta potential data also showed a statistically significant increase in zeta potential at 0.05% BSA which corresponds to the increase in plasma membrane binding observed in the plate reader data (Figure 14).

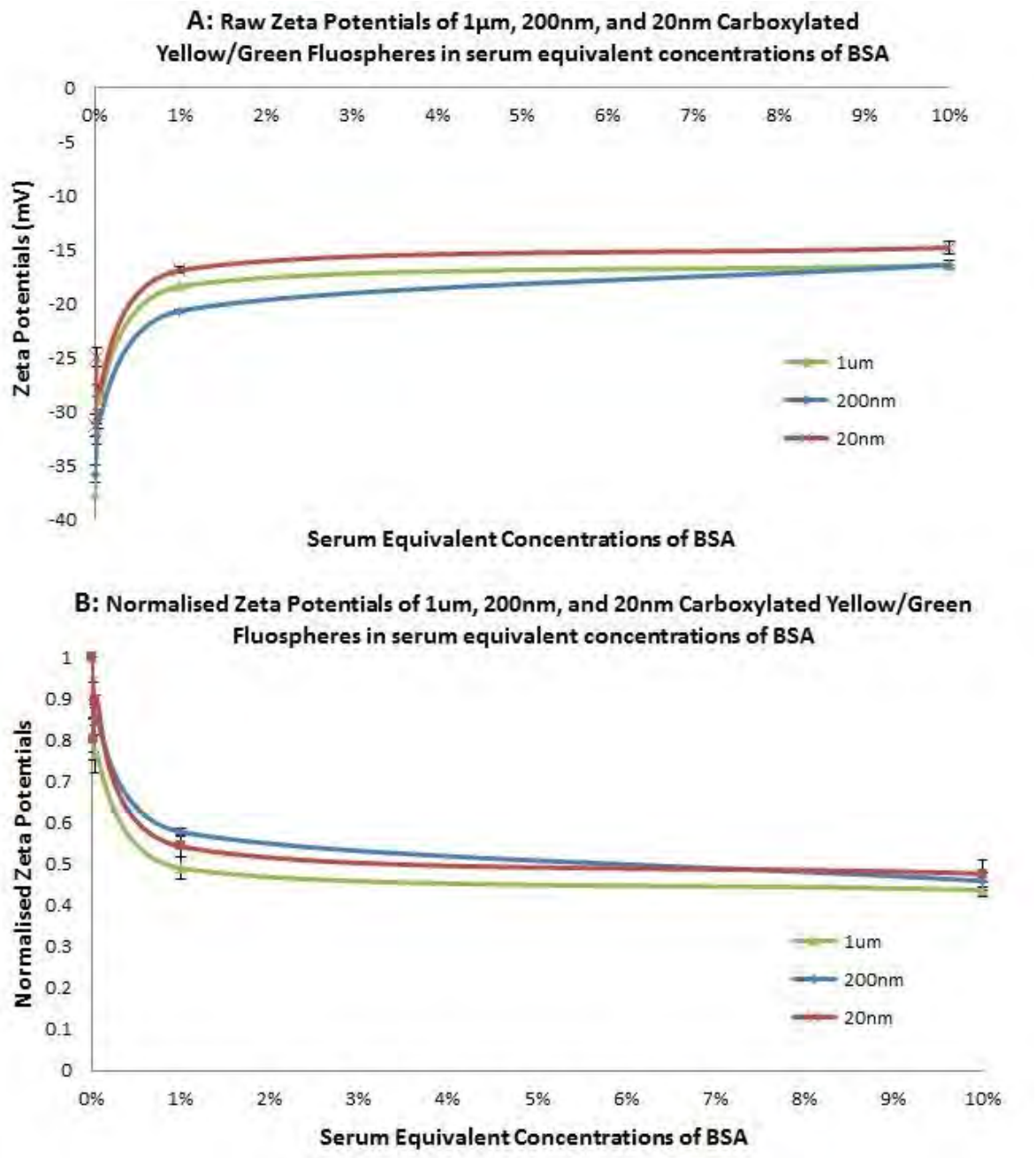

Figure 16 A) Raw zeta potential data for 1µm, 20nm, and 200nm carboxylate modified yellow/green polystyrene FluoSpheres in serum equivalent concentrations of Bovine Serum Albumin (BSA). The data shows an exponential decay in zeta potential for all three particles tested. B) Normalised zeta potential data shows that the reduction in zeta potential is uniform across all three sizes, and the only statistically significant data point (after a t-test to compare 20nm data with 200nm and 1µm measurements) is at 0.05%. (Error bars indicate standard error of the mean).

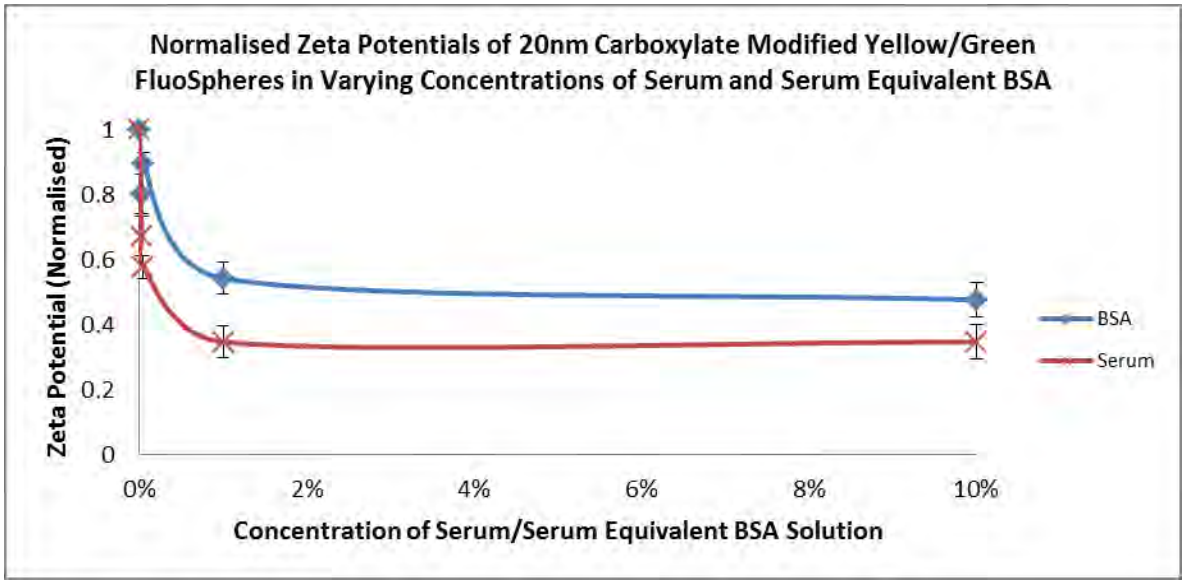

Figure 17 Graph comparing the reduction in zeta potentials (normalised) of 20nm carboxylate modified yellow/green polystyrene nanoparticles in the presence of different concentrations of serum and bovine serum albumin (BSA). The concentrations of BSA reported are in proportion to the amounts of BSA found in equivalent concentrations of serum, therefore 2% BSA is equivalent to the amount of BSA found in 2% serum. A) The graph shows that while BSA causes a reduction of Zeta potential, the magnitude of this change is not equivalent to the reduction in zeta potential induced by serum (all results statistically significant with $p < 0.05$). (Error bars indicate standard error of the mean).

3.5 Washes to Remove Membrane Bound Polystyrene Nanoparticles

As described in Section 2.5, a number of different methods were used to attempt to remove plasma membrane bound nanoparticles. The successful removal of all surface bound fluorescence would allow for the accurate quantification and study of nanoparticle internalisation under different conditions and contribute to an improved understanding of the mechanisms of nanoparticle entry into cells in the context of different biological media.

Unfortunately none of the attempted protocols successfully removed all of the surface bound 20nm carboxylate modified yellow/green polystyrene nanoparticles. The results of the most successful attempt are shown in Figure 18, where a series of successive 5 minute Hank's Balanced Salt Solution (HBSS) and 30 second Accutase washes were used.

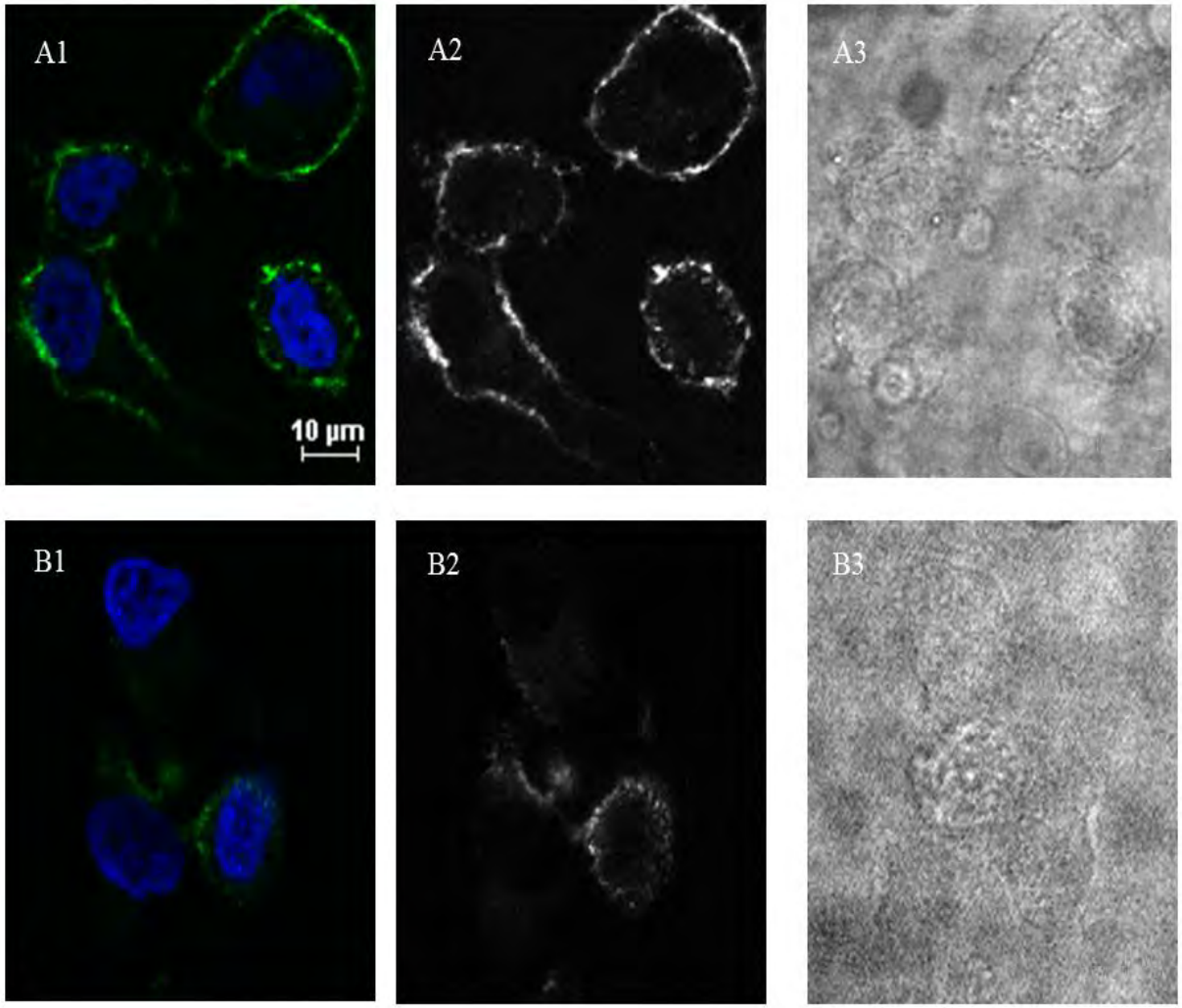

Figure 18 Confocal microscopy images of cells treated with a 1:1000 dilution of 20nm carboxylate modified yellow/green polystyrene nanoparticles in serum free Dulbecco's Modified Eagle's Media (DMEM) for 15 minutes. Images A1-3 represent control cells which show that at 15 minutes nanoparticles are bound to the plasma membrane. A1 shows cells with both green (polystyrene nanoparticles) and blue (DAPI nuclear stain signal), while A2 shows the same image on the green filter scaled for brightness. A3 is a transmitted light image for comparison. Images B1-3 show cells treated with nanoparticles as in A which were then treated with 4 successive 5 minute Hank's Balanced Salt Solution (HBSS) and 30 second Accutase washes. Images B1 and B2 show significantly reduced fluorescence from membrane bound nanoparticles when compared to the control images (A1 and A2), however some membrane associated signal remains.

SECTION 4: DISCUSSION

4.1.1 Membrane Binding and Zeta Potentials in Serum

The effect of serum on nanoparticle binding to the plasma membrane was found to be dependent on serum concentration and the size of the polystyrene FluoSpheres used. For all three sizes of carboxylate modified polystyrene particles studied, the membrane associated signal decreased in response to an increasing concentration of serum. This effect was diminished as the polystyrene FluoSpheres increased in size, with 20nm nanoparticles showing the greatest sensitivity to the inhibitory effect of serum, while 200nm and 1μm particle binding to the plasma membrane were successively less affected.

The reduction in membrane binding caused by serum is attributed to the formation of a protein corona around nanoparticles, and size has been shown to be an important factor in driving both the composition and kinetics of protein binding to nanoparticles (Jiang *et al.* 2008; Walkey *et al.* 2012). This data further supports existing evidence that shows that particle size strongly influences the formation of a protein corona, and its consequent inhibition of interactions between nanoparticles and cells (Walkey *et al.* 2012). Moreover the fact that there is a clear relationship between membrane binding and the concentration of serum indicates that protein abundance is also an important factor in corona formation and the resultant effects on nanoparticle-plasma membrane binding.

Interestingly the zeta potential data presented in this study showed that size had no significant effect on the reduction of surface charge caused by the formation of a protein

corona. All three sizes tested in this study exhibited the same sharp decrease in zeta potential at low concentrations of serum, an effect which plateaued rapidly in contrast to the plasma membrane binding data which showed a much smaller decay constant, and did not reach saturation even at the highest tested concentration of serum (10%).

The homogenous change in zeta potential observed between particles of different sizes could be attributed to the fact that the concentrations of the differently sized nanoparticles used were scaled to ensure that the total available surface area for protein interactions was constant.

The zeta potential data reported in this study suggests that at approximately 1% serum (above which surface charge remains relatively constant) there is sufficient material in the test solutions to form a stable corona, and that the total quantity of nanoparticle bound protein remains constant despite the increase in serum, and hence protein, concentration. The plate reader data however shows that the inhibitory effect of serum on nanoparticle-cell interactions continues to increase above 1%, and does not reach a saturation point even at the highest test concentration.

In light of the current model of corona formation described by the Vroman Effect (Section 1.5.1), it can be hypothesised that while above 1% the total quantity of protein forming the corona remains constant, the composition of the corona in terms of the identity of the proteins bound continues to be affected by the changing abundance of protein in the test solutions (Sanfins *et al.* 2011; Casals *et al.* 2010).

This hypothesis is supported by a study performed by Monopoli *et al.* (2011) into the effects of varying concentrations of plasma on the composition of the protein corona. The authors found that the proteins making up the corona in these different conditions would vary. This suggests that protein abundance in biological media impact the kinetics of their adsorption onto nanoparticles, and hence, the composition of the corona formation and any consequent physiological response (Monopoli *et al.* 2011).

While the importance of size, shape, and surface chemistry on corona formation has been clearly illustrated, the role that variations in biological media in terms of, for example, protein abundance, has yet to be sufficiently investigated (Nel *et al.* 2009; Walkey and Chan 2011). This is a particularly relevant area of study in light of the fact that there are diverse biological media to which nanoparticles can be exposed *in vivo*. For example, particulate matter in the atmosphere would be exposed to mucosa in the respiratory tract, while nanoparticles administered medically are more likely to be exposed to plasma (Abdelhalim and Jarrar 2012).

Similarly understanding how variations in physiological environments affect nanoparticle behaviours *in vivo* is particularly relevant to designing and administering nanotherapies (Petros and DeSimone 2010). Understanding variations in corona formation dependent on the media to which nanoparticles are exposed could inform clinical decisions regarding routes of administration which would ultimately affect the effectiveness of such therapies (Petros and DeSimone 2010).

4.1.2 Future Work

As discussed in Section 4.1.1, the zeta potential and plate reader data reported in this study suggest that while a stable corona forms around nanoparticles at approximately 1% (resulting in the observed stable reduction in zeta potential), the composition of said corona changes in response to further increases in serum concentration. To investigate this hypothesis, further work establishing which proteins form the corona at different concentrations of serum is needed. Proteomic approaches like mass spectroscopy have proven to be powerful tools in determining which proteins bind nanoparticles in biological solutions (Lundqvist *et al.* 2008).

Surface charge has been shown to be one of the main factors driving protein binding and corona formation (Patil *et al.* 2007; Casals *et al.* 2010). As such further study into the effects of serum into positively charged polystyrene particles would provide further insight into the role of charge in nanoparticle interactions with plasma membranes and serum proteins. Similarly, investigating particles of equivalent size and surface chemistry but differing physicochemical composition (e.g. gold or iron oxide) would demonstrate whether composition plays as significant a role in protein interactions in serum as surface chemistry and size (Deng *et al.* 2009).

Plasma and mucosa are two physiological fluids to which nanoparticles are exposed both as potentially harmful agents in the atmosphere and as medical vehicles for treatment, and as such characterising their effects on particles of different sizes is an important aspect of modelling how nanoparticles behave *in vivo* (Hyun *et al.* 2008; Monopoli *et al.* 2011). As

such investigations into the effects of these media at varying concentrations on nanoparticle-cell interactions and surface charge could be interesting and highly relevant areas of study.

Similarly studying these effects in tissue types relevant to routes of exposure is also important to understanding nanoparticle-cell interactions in the context of their use and real life exposure (McCall 2011). Primary cell types like lung epithelium and liver cells are good examples of important tissue types to which nanoparticles would be exposed, and reproducing the effects reported in this study in these cell types would make this work more relevant to existing toxicological concerns (Abdelhalim and Jarrar 2012; Limbach *et al.* 2007).

4.2.1 Membrane Binding and Zeta Potentials in Bovine Serum Albumin

The plasma membrane binding and zeta potential experiments were repeated in Bovine Serum Albumin (BSA), the most abundant protein in serum and in human plasma, to determine whether the inhibitory effect of serum on nanoparticle-plasma membrane binding could be reproduced with BSA alone. The data shows that while a size- and concentration dependent reduction in both membrane binding and surface charge are evident, this change is not of the same magnitude as the serum induced effect.

This finding is particularly relevant in terms of experimental design as a number of recently published studies use BSA in isolation in studies modelling protein adsorption and corona

formation. Patil *et al.* (2007) for example investigate the effects of biological media on the uptake and surface charge of cerium oxide using BSA solutions.

This use of BSA is based on the assumption that as the most abundant protein in plasma and serum, albumin plays a key role in the formation and effects of the protein corona. This is supported by proteomic studies conveniently summarised by Walkey and Chan (2011) (Figure 8) who show that 24 of 26 investigations quantifying the composition of the corona detected albumin in the protein corona.

However, as the data reported in this study shows, the effects of BSA on surface charge and polystyrene nano- and microsphere binding to the plasma membrane are not directly comparable to the effects of serum in equivalent conditions.

A reproducible but not statistically significant increase in membrane binding was observed at low concentrations of BSA for all three polystyrene FluoSpheres tested. Interestingly a statistically significant increase in zeta potential was observed when 20nm polystyrene nanoparticles were immersed in 0.05% BSA. This effect was not observed at any other concentration or particle size.

Particular concentrations of plasma and serum have been shown to stabilise certain nanomaterials in biological media, causing them to disaggregate and thereby making more binding sites available for cell interactions (Wiogo *et al.* 2011; Monopoli *et al.* 2011). This effect has been shown by Wiogo *et al.* (2011) who found that magnetic iron oxide particles in high concentrations of Foetal Bovine Serum (FBS) disaggregated to yield particles with a significantly smaller hydrodynamic diameter than controls (Figure 19).

This phenomenon has thus far proven to be nanomaterial dependent as it has not been observed in sulfonated polystyrene nanoparticles in a study by Monopoli *et al.* (2011) into the effects of varying plasma concentrations on corona formation.

One of the major concerns in the area of designing nanomaterials for biomedical use is aggregation *in vivo* (Wiogo *et al.* 2011). Large aggregates can potentially induce an immune response, reducing the circulation time of drug delivery vectors (Fukumori and

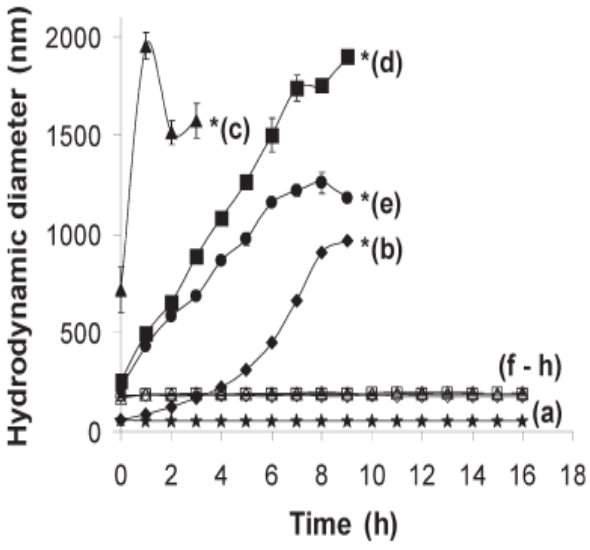

Figure 19 Image showing the average hydrodynamic diameter of magnetic iron nanoparticles in a number of different media. The lowest hydrodynamic diameter observed was in a) water, f) 4%, g) 8%, and h) 10% Foetal Bovine Serum (FBS). At these concentrations FBS stabilised the iron nanoparticles tested, causing them to disaggregate. At lower concentrations of FBS (c) 0%, d) 1%, e) 2% FBS) and in b) phosphate-buffered saline (PBS) particles would aggregate resulting in the large hydrodynamic radius observed by dynamic light scattering (DLS) (Image from Wiogo *et al.* 2011).

Ichikawa 2006). Particularly large aggregates in the region of 4μm diameters can also potentially cause the blockage of fine blood capillaries (Neuberger *et al.* 2005). As Wiogo *et al.* (2011) have shown however, it is possible to stabilise particular nanomaterials via the adsorption of BSA and the subsequent disaggregation of particles. The magnetic nanoparticles tested by Wiogo *et al.* (2011) remained in a disaggregated state once immersed in biological media after treatment with BSA, suggesting that this method is a potential solution to the problem of unwanted aggregation *in vivo.*

In this study we have observed a trend which indicates that particular concentrations of BSA can stabilise polystyrene FluoSpheres of various sizes, and that the stabilising effect of BSA observed by Wiogo *et al.* could potentially be reproduced in other nanomaterials.

4.2.2 Future Work

As discussed in Section 4.2, an increase in plasma membrane associated signal was observed at low concentrations of BSA, an effect which can potentially be attributed to a previously observed 'stabilising' effect of protein corona which can cause particle disaggregation (Wiogo *et al.* 2011).

To test this hypothesis reliable sizing data would be needed to determine whether the increase in plasma membrane binding correlates to a disaggregation of polystyrene FluoSpheres at low concentrations of BSA. While Dynamic Light Scattering (DLS) has traditionally been used for nanoparticle sizing, its use is more appropriate for

monodispersed samples where an average hydrodynamic diameter is reflective of individual particle sizes (Poda *et al.* 2011).

In this instance the presence of aggregates of different sizes warrant the use of a technique like Field Flow Fractionation (FFF), which separates a suspension of nanoparticles according to size to yield data on the differently sized aggregates present in a particular test solution (Poda *et al.* 2011). Investigating the sizes of aggregates at low concentrations of BSA would prove an effective way to test the hypothesis that these amounts of protein can cause the disaggregation of particles which would result in increased nanoparticle-membrane interactions.

Sizing data for both the BSA and serum data would also prove useful in light of the important consequences of nanoparticle aggregation *in vivo* (Gosens *et al.* 2010). As discussed in Section 4.2.1, large aggregates can cause capillary blockages and induce an immune response (Fukumori and Ichikawa 2006; Neuberger *et al.* 2005), and as such understanding how serum and BSA concentrations affect nanoparticle aggregation is relevant to accurately modelling nanoparticle behaviours in physiological environments (Walkey and Chan 2011).

4.3.1 Washes to Remove Membrane Bound Nanoparticles

A number of different conditions were used in an attempt to remove membrane nanoparticles and allow for the study of nanoparticle internalisation through the plate reader assay used in this study. The ice cold Hank's Balanced Salt Solution (HBSS) washes

performed by Georgieva *et al.* (2010) did not successfully remove all of the membrane bound signal upon analysis with a Nikon inverted A1R confocal microscope.

Trypsin washes proved effective after 60 second washes, however these washes would cause cells to detach and were therefore not applicable for the purposes of this study. As shown in Section 3.5, the most effective protocol proved to be a series of 5 minute HBSS washes and 30 second incubations with an alternative protease, Accutase. However even this method did not completely remove the membrane bound signal, and in order for a study of nanoparticle internalisation to be performed using the plate reader study a protocol is needed that would effectively remove 100% of membrane bound nanoparticles.

4.3.2 Future Work

As the most dramatic removal of membrane bound nanoparticles was achieved by 4 rounds of 5 minute HBSS washes followed by 30 seconds of Accutase, future development of this protocol should investigate using more extensive washes to remove the last of the membrane associated signal. Using 5 or 6 rounds of washes for example could prove successful.

SECTION 5: CONCLUDING REMARKS

In this study the relationship between serum and its resultant effects on surface charge and the binding of polystyrene nanoparticles to the plasma membrane has been investigated. The previously reported inhibitory effect of serum on polystyrene nanoparticle interactions with the plasma membrane has been shown to depend on both the concentration of serum and the size of the particles in question.

Furthermore the reduction in zeta potential evidenced by the formation of a protein corona was shown to affect particles of all three sizes investigated equally. The data to hand suggests that a stable corona forms at a relatively low concentration of serum (approximately 1%), while the reduction in plasma membrane binding induced by the corona continues to increase as the concentration of serum increases. This finding warrants further investigation into the proteins adsorbing to the polystyrene FluoSpheres tested, and how the composition of the corona changes in response to changing protein abundance.

Bovine serum albumin (BSA) in concentrations equivalent to those found in serum did not reproduce the effect observed in the presence of serum. However an observation of interest was an increase in membrane-associated signal at low concentrations of BSA, a finding which could be attributed to the potential disaggregation of particles in these conditions.

Understanding how the presence of biological media affects nanoparticle interactions with cells and tissues is a matter of concern as exposure to nanomaterials through various routes increases (McCall 2011). The findings reported in this study contribute to a deeper

understanding of how factors like particle size, protein abundance, and surface charge affect nanoparticle interactions with cells.

SECTION 6: REFERENCES

Abdelhalim, M.A.K. & Jarrar, B.M., 2012. Histological alterations in the liver of rats induced by different gold nanoparticle sizes, doses and exposure duration. ***Journal of Nanobiotechnology***, 10(1), p.5.

Apel, K. & Hirt, H., 2004. Reactive oxygen species: metabolism, oxidative stress, and signal transduction. ***Annual Review of Plant Biology***, 55, pp.373-399.

Aubin-Tam, M.E. & Hamad-Schifferli, K., 2005. Gold nanoparticle-cytochrome c complexes: the effect of nanoparticle ligand charge on protein structure. ***Langmuir***, 21(26), pp.12080-12084.

Ayres, J.G. et al., 2008. Evaluating the toxicity of airborne particulate matter and nanoparticles by measuring oxidative stress potential-a workshop report and consensus statement. ***Inhalation toxicology***, 20(1), pp.75-99.

BéruBé, K. et al., 2007. Combustion-Derived Nanoparticles: Mechanism of Pulmonary Toxicity. ***Clinical and Experimental Pharmacology and Physiology***, 34(10), pp.1044-1050.

Canagaratna, M.R. et al., 2010. Evolution of vehicle exhaust particles in the atmosphere. ***Journal of the Air & Waste Management Association***, 60(10), pp.1192-1203.

Casals, E. et al., 2010. ***Time evolution of the nanoparticle protein corona***. ACS nano, 4(7), pp.3623-3632.

Cedervall, T., Lynch, I., Foy, M., et al., 2007. Detailed identification of plasma proteins adsorbed on copolymer nanoparticles. ***Angewandte Chemie International Edition***, 46(30), pp.5754-5756.

Cedervall, T., Lynch, I., Lindman, S., et al., 2007. Understanding the nanoparticle-protein corona using methods to quantify exchange rates and affinities of proteins for nanoparticles. ***Proceedings of the National Academy of Sciences***, 104(7), p.2050.

Chakraborty, S. et al., 2011. Contrasting Effect of Gold Nanoparticles and Nanorods with Different Surface Modifications on the Structure and Activity of Bovine Serum Albumin. ***Langmuir***, 27, pp. 7722-7731.

Cho, W.S. et al., 2009. Acute toxicity and pharmacokinetics of 13 nm-sized PEG-coated gold nanoparticles. ***Toxicology and applied pharmacology***, 236(1), pp.16-24.

Clift, M.J.D. et al., 2008. The impact of different nanoparticle surface chemistry and size on uptake and toxicity in a murine macrophage cell line. ***Toxicology and applied pharmacology***, 232(3), pp. 418-427.

Clift, M.J.D. et al., 2010. The effects of serum on the toxicity of manufactured nanoparticles. ***Toxicology letters***, 198(3), pp.358-365.

Dankovich, T.A. & Gray, D.G., 2011. Bactericidal paper impregnated with silver nanoparticles for point-of-use water treatment. ***Environmental science & technology***, 54, pp. 1992-1998.

De, M. et al., 2007. Biomimetic interactions of proteins with functionalized nanoparticles: a thermodynamic study. ***Journal of the American Chemical Society***, 129(35), pp.10,747-10,753.

Dell'Orco, D. et al., 2010. Modeling the time evolution of the nanoparticle-protein corona in a body fluid. ***PloS one***, 5(6), p.e10949.

Deng, Z.J. et al., 2009. Differential plasma protein binding to metal oxide nanoparticles. ***Nanotechnology***, 20, p.455101.

Duncan, T.V., 2011. The communication challenges presented by nanofoods. ***Nature Nanotechnology***, 6(11), pp.683-688.

Fukumori, Y., Ichikawa, H., 2006. ***Advanced Powder Technology***, 17, pp. 1–28.

Fushimi, A. et al., 2011. Organic-rich nanoparticles (diameter: 10-30 nm) in diesel exhaust: Fuel and oil contribution based on chemical composition. ***Atmospheric Environment***, 45(35), pp.6326-6336.

Georgieva, J.V. et al., 2010. Surface characteristics of nanoparticles determine their intracellular fate in and processing by human blood-brain barrier endothelial cells in vitro. ***Molecular Therapy***, 19(2), pp.318-325.

Gessner, A. et al., 2000. Nanoparticles with decreasing surface hydrophobicities: influence on plasma protein adsorption. ***International Journal of Pharmaceutics***, 196(2), pp.245-249.

Ghosh, P. et al., 2008. Gold nanoparticles in delivery applications. ***Advanced Drug Delivery Reviews***, 60(11), pp.1307-1315.

Goodman, C.M. et al., 2004. Toxicity of gold nanoparticles functionalized with cationic and anionic side chains. ***Bioconjugate Chemistry***, 15(4), pp.897-900.

Gosens I, Post J.A., et al., 2010. Impact of Agglomeration State of Nano- and Submicron Sized Gold Particles on Pulmonary Inflammation. ***Part Fibre Toxicology***, 2, pp. 7-37.

Grahame, T.J. & Schlesinger, R.B., 2012. Oxidative Stress-Induced Telomeric Erosion as a Mechanism Underlying Airborne Particulate Matter-Related Cardiovascular Disease. ***Particle and Fibre Toxicology,*** 9(1), p.21.

Green, R. et al., 1999. Competitive protein adsorption as observed by surface plasmon resonance. ***Biomaterials***, 20(4), pp.385-391.

Greish, K., 2011. Enhanced permeability and retention effect for selective targeting of anticancer nanomedicine: are we there yet? ***Drug Discovery Today: Technologies,*** doi:10.1016/j.ddtec.2011.11.010.

Gupta, A.K. et al., 2007. Recent advances on surface engineering of magnetic iron oxide nanoparticles and their biomedical applications. ***Nanomedicine***, 2(1), pp.23-39.

Harisinghani, M.G. et al., 2003. Noninvasive detection of clinically occult lymph-node metastases in prostate cancer. ***New England Journal of Medicine***, 348(25), pp.2491-2499.

Heitbrink W.A., Evans D.E., Peters T.M., Slavin T.J., 2007. Characterization and Mapping of Very Fine Particles in an Engine Machining and Assembly Facility. ***Journal of Occupational and Environmental Hygiene,*** 4(5), pp. 341-351.

Heng, B.C. et al., 2010. Toxicity of zinc oxide (ZnO) nanoparticles on human bronchial epithelial cells (BEAS-2B) is accentuated by oxidative stress. ***Food and Chemical Toxicology***, 48(6), pp.1762-1766.

Hillie, T. & Hlophe, M., 2007. Nanotechnology and the challenge of clean water. ***Nature Nanotechnology***, 2(11), pp.663-664.

Hong, R. et al., 2004. Control of protein structure and function through surface recognition by tailored nanoparticle scaffolds. ***Journal of the American Chemical Society***, 126(3), pp.739-743.

Hyun, J.S. et al., 2008. Effects of repeated silver nanoparticles exposure on the histological structure and mucins of nasal respiratory mucosa in rats. ***Toxicology Letters,*** 182(1-3), pp.24-28.

Instruments, M., 2004. Zetasizer nano series user manual. Worcestershire: Malvern Instruments Ltd.

Jiang, W. et al., 2008. Nanoparticle-mediated cellular response is size-dependent. ***Nature Nanotechnology***, 3(3), pp.145-150.

Keskinen, J. & Rönkkö, T., 2010. Can Real-World Diesel Exhaust Particle Size Distribution be Reproduced in the Laboratory? A Critical Review Jorma Keskinen. ***Journal of the Air & Waste Management Association***, 60(10), pp.1245-1255.

Kim, J.S. et al., 2006. Toxicity and tissue distribution of magnetic nanoparticles in mice. ***Toxicological Sciences***, 89(1), pp.338-347.

Kostarelos, K., Bianco, A. & Prato, M., 2009. Promises, facts and challenges for carbon nanotubes in imaging and therapeutics. ***Nature Nanotechnology***, 4(10), pp.627-633.

Lee, S.H. et al., 2012. Toxic response of zinc oxide nanoparticles in human epidermal keratinocyte HaCaT cells. ***Toxicology and Environmental Health Sciences***, 4(1), pp.14-18.

Li, N., Xia, T. & Nel, A.E., 2008. The role of oxidative stress in ambient particulate matter-induced lung diseases and its implications in the toxicity of engineered nanoparticles. ***Free Radical Biology and Medicine***, 44(9), pp.1689-1699.

Li, W. et al., 2011. Gold nanocages as contrast agents for photoacoustic imaging. ***Contrast Media & Molecular Imaging***, 6(5), pp.370-377.

Li, Y.F. & Chen, C., 2011. Fate and Toxicity of Metallic and Metal-Containing Nanoparticles for Biomedical Applications. ***Small***, 2(21), pp. 2965-2980.

Libutti, S.K. et al., 2010. Phase I and pharmacokinetic studies of CYT-6091, a novel PEGylated colloidal gold-rhTNF nanomedicine. ***Clinical Cancer Research***, 16(24), pp.6139-6149.

Limbach, L.K. et al., 2007. Exposure of engineered nanoparticles to human lung epithelial cells: influence of chemical composition and catalytic activity on oxidative stress. ***Environmental Science & Technology***, 41(11), pp.4158-4163.

Llevot, A. & Astruc, D., 2011. Applications of vectorized gold nanoparticles to the diagnosis and therapy of cancer. ***Chemical Society Review***, 41(1), pp.242-257.

Lorenz, C, *et al.* Characterization of silver release from commercially available functional (nano)textiles. ***Chemosphere*** (2012), http://dx.doi,org/10.10160/j.chemosphere.2012.04.063.

Lorenz, C. et al., 2012. Characterization of silver release from commercially available functional (nano) textiles. ***Chemosphere***, http://dx.doi.org/10.1016/j.chemosphere.2012.04.063.

Lota, G., Fic, K. & Frackowiak, E., 2011. Carbon nanotubes and their composites in electrochemical applications. ***Energy and Environmental Science***., 4(5), pp.1592-1605.

Love, S.A., Thompson, J.W. & Haynes, C.L., 2012. Development of screening assays for nanoparticle toxicity assessment in human blood: preliminary studies with charged Au nanoparticles. ***Nanomedicine***, (0), pp.1-10.

Lovern, S.B. & Klaper, R., 2006. Daphnia magna mortality when exposed to titanium dioxide and fullerene (C60) nanoparticles. ***Environmental Toxicology and Chemistry***, 25(4), pp.1132-1137.

Lundqvist, M. et al., 2008. Nanoparticle size and surface properties determine the protein corona with possible implications for biological impacts. Proceedings of the ***National Academy of Sciences***, 105(38), p.14265.

Lynch, I. & Dawson, K.A., 2008. Protein-nanoparticle interactions. **Nano Today**, 3(1), pp.40-47.

Lynch, I. et al., 2007. The nanoparticle-protein complex as a biological entity; a complex fluids and surface science challenge for the 21st century. **Advances in Colloid and Interface Science**, 134, pp.167-174.

Lynch, I., Salvati, A. & Dawson, K.A., 2009. Protein-nanoparticle interactions: What does the cell see? ***Nature Nanotechnology***, 4, pp.546-547.

Ma, H.L. et al., 2008. Magnetic targeting after femoral artery administration and biocompatibility assessment of superparamagnetic iron oxide nanoparticles. ***Journal of Biomedical Materials Research,*** Part A, 84(3), pp.598-606.

Mahmoudi, M. et al., 2011. Irreversible changes in protein conformation due to interaction with superparamagnetic iron oxide nanoparticles. ***Nanoscale***, 3(3), pp.1127-1138.

Maneerung, T., Tokura, S. & Rujiravanit, R., 2008. Impregnation of silver nanoparticles into bacterial cellulose for antimicrobial wound dressing. ***Carbohydrate Polymers***, 72(1), pp.43-51.

McCall, M.J., 2011. Environmental, health and safety issues: Nanoparticles in the real world. ***Nature Nanotechnology***, 6(10), pp.613-614.

Monopoli, M.P. et al., 2011. Physical- Chemical Aspects of Protein Corona: Relevance to in Vitro and in Vivo Biological Impacts of Nanoparticles. ***Journal of the American Chemical Society***, 133, pp. 2525–2534

Murray, A.R. et al., 2012. Oxidative Stress and Dermal Toxicity of Iron Oxide Nanoparticles *In Vitro*. ***Cell Biochemistry and Biophysics***, pp.1-16.

Nel, A.E. et al., 2009. Understanding biophysicochemical interactions at the nano-bio interface. ***Nature Materials***, 8(7), pp.543-557.

Neuberger T., Schopf B., Hofmann H., *et al.*, 2005. Superparamagnetic nanoparticles for biomedial applications: Possibilities and limitations of a new drug delivery system. ***Journal of Magnetism and Magnetic Materials***, 293, pp. 483–496.

Nohynek, G.J. & Dufour, E.K., 2012. Nano-sized cosmetic formulations or solid nanoparticles in sunscreens: A risk to human health? ***Archives of Toxicology***, pp.1-13.

Ohkoshi S.I., Tsunobuchi Y., Matsuda T., Hashimoto K., *et al.,* 2010. Synthesis of a metal oxide with a room-temperature photoreversible phase transition. ***Nature Chemistry,*** 2, pp. 539-545.

Pan, Y. et al., 2007. Size-Dependent Cytotoxicity of Gold Nanoparticles. ***Small***, 3(11), pp.1941-1949.

Park, E.J. et al., 2008. Oxidative stress and apoptosis induced by titanium dioxide nanoparticles in cultured BEAS-2B cells. ***Toxicology Letters***, 180(3), pp.222-229.

Patil, S. et al., 2007. Protein adsorption and cellular uptake of cerium oxide nanoparticles as a function of zeta potential. ***Biomaterials***, 28(31), pp.4600-4607.

Petros A.P., DeSimone J.M., 2010. Strategies in the design of nanoparticles for therapeutic applications. ***Nature Reviews Drug Discovery***, 9, pp. 615-627.

Pinnell, S.R. et al., 2000. Microfine zinc oxide is a superior sunscreen ingredient to microfine titanium dioxide. ***Dermatologic Surgery***, 26(4), pp.309-314.

Poda, A. et al., 2010. Characterization of silver nanoparticles using flow-field flow fractionation interfaced to inductively coupled plasma mass spectrometry. ***Journal of Chromatography A***, 1218 (2011), pp. 4219– 4225.

Rejman, J. et al., 2004. Size-dependent internalization of particles via the pathways of clathrin-and caveolae-mediated endocytosis. ***Biochemical Journal***, 377(Pt 1), pp.159-169.

Revell, P., 2006. The biological effects of nanoparticles. ***Nanotechnology Perceptions***, 2, pp.283-298.

Rice W.R, 1989. Analyzing Tables of Statistical Tests. ***Society for the Study of Evolution***, 43(1), pp.223-225.

Roach, P., Farrar, D. & Perry, C.C., 2006. Surface tailoring for controlled protein adsorption: effect of topography at the nanometer scale and chemistry. ***Journal of the American Chemical Society***, 128(12), pp. 3939-3945.

Ruge, C.A. et al., 2011. Uptake of nanoparticles by alveolar macrophages is triggered by surfactant protein A. ***Nanomedicine: Nanotechnology, Biology and Medicine***, 7, pp.690-693.

Sakurai, H. et al., 2003. On-line measurements of diesel nanoparticle composition and volatility. ***Atmospheric Environment***, 37(9-10), pp.1199-1210.

Sanfins, E. et al., 2011. Nanoparticle-protein interactions: from crucial plasma proteins to key enzymes. ***Journal of Physics: Conference Series***, 304, pp.012-039.

Schneider, G. et al., 2006. Distance-dependent fluorescence quenching on gold nanoparticles ensheathed with layer-by-layer assembled polyelectrolytes. ***Nano Letters***, 6(3), pp.530-536.

Seo, Y. I *et al.* Removal of bacterial pathogen from wastewater using AI filter with Ag-containing nano-composite film by *in situ* dispersion involving polyol process, ***Journal of Hazardous Materials*** (2012), http://dx.doi.org.10.1016/j.jhazmat.2012.05.026.

Seo, Y.I. et al., 2012. Removal of bacterial pathogen from wastewater using Al filter with Ag-containing nanocomposite film by *in situ* dispersion involving polyol process. ***Journal of Hazardous Materials,*** http://dx.doi.org/10.1016/j.jhazmat.2012.05.026.

Shang, W. et al., 2007. Unfolding of ribonuclease A on silica nanoparticle surfaces. ***Nano Letters***, 7(7), pp.1991-1995.

Sharma, V. et al., 2009. DNA damaging potential of zinc oxide nanoparticles in human epidermal cells. ***Toxicology Letters***, 185(3), pp.211-218.

Sharma, V., Anderson, D. & Dhawan, A., 2012. Zinc oxide nanoparticles induce oxidative DNA damage and ROS-triggered mitochondria mediated apoptosis in human liver cells (HepG2). ***Apoptosis***, pp.1-19.

Siddiqi, N.J. et al., 2012. Identification of potential biomarkers of gold nanoparticle toxicity in rat brains. ***Journal of Neuroinflammation***, 9(1), p.123.

Smith, P.J. et al., 2012. Cellular entry of nanoparticles via serum sensitive clathrin-mediated endocytosis, and plasma membrane permeabilization. ***International Journal of Nanomedicine***, 7, pp.2045-2055.

Song, Y., Li, X. & Du, X., 2009. Exposure to nanoparticles is related to pleural effusion, pulmonary fibrosis and granuloma. ***European Respiratory Journal***, 34(3), pp.559-567.

Thornburg J., Leith A., 2000. Size distribution of mist generated during metal machining. ***Applied Occupational Environmental Hygiene***, 15(8): 618-28.

Tobias, H.J. et al., 2001. Chemical analysis of diesel engine nanoparticles using a nano-DMA/thermal desorption particle beam mass spectrometer. ***Environmental Science & Technology***, 35(11), pp.2233-2243.

Trouiller, B. et al., 2009. Titanium dioxide nanoparticles induce DNA damage and genetic instability in vivo in mice. ***Cancer Research***, 69(22), p.8784.

Van Berlo, D. et al., 2010. Comparative evaluation of the effects of short-term inhalation exposure to diesel engine exhaust on rat lung and brain. ***Archives of toxicology***, 84(7), pp.553-562.

Verma, A. & Stellacci, F., 2010. Effect of surface properties on nanoparticle-cell interactions. ***Small***, 6(1), pp.12-21.

Walkey, C.D. & Chan, W.C.W., 2011. Understanding and controlling the interaction of nanomaterials with proteins in a physiological environment. ***Chemical Society Review,*** 41, pp. 2780–2799.

Walkey, C.D. et al., 2012. Nanoparticle size and surface chemistry determine serum protein adsorption and macrophage uptake. ***Journal of the American Chemical Society***, 134(4), p.2139.

Wang, Y.F. et al., 2011. Size distributions and exposure concentrations of nanoparticles associated with the emissions of oil mists from fastener manufacturing processes. ***Journal of Hazardous Materials***. 198, pp. 182– 187.

Weir, A. et al., 2012. Titanium Dioxide Nanoparticles in Food and Personal Care Products. ***Environmental Science & Technology***. 198, pp. 182– 187.

Wiogo, H.T.R. et al., 2011. Stabilization of magnetic iron oxide nanoparticles in biological media by fetal bovine serum (FBS). ***Langmuir***. 27(2), pp. 843–850

Xia, T. et al., 2008. Comparison of the mechanism of toxicity of zinc oxide and cerium oxide nanoparticles based on dissolution and oxidative stress properties. ***ACS Nano***, 2(10), pp.2121-2134.

Yang, W. et al., 2010. Carbon nanomaterials in biosensors: should you use nanotubes or graphene? ***Angewandte Chemie International Edition***, 49(12), pp.2114-2138.

Yu, J., Ma, T. & Liu, S., 2011. Enhanced photocatalytic activity of mesoporous TiO2 aggregates by embedding carbon nanotubes as electron-transfer channel. ***Physical Chemistry Chemical Physics***, 13(8), pp.3491-3501.

Zhang, F. et al., 2009. Application of silver nanoparticles to cotton fabric as an antibacterial textile finish. ***Fibers and Polymers***, 10(4), pp.496-501.

Zhang, H., Burnum, K.E., et al., 2011. Quantitative proteomics analysis of adsorbed plasma proteins classifies nanoparticles with different surface properties and size. ***Proteomics***, 11(4569-4577).

Zhang, X.D. et al., 2010. Toxicologic effects of gold nanoparticles in vivo by different administration routes. ***International Journal of Nanomedicine***, 5, p.771-781.

Zhang, X.D. et al., 2012. *In vivo* renal clearance, biodistribution, toxicity of gold nanoclusters. ***Biomaterials***. 33, pp. 4628-4638.

Zhang, X.D., Wu, D., et al., 2011. Size-dependent in vivo toxicity of PEG-coated gold nanoparticles. ***International Journal of Nanomedicine***, 6, p.2071-2081.

Zhu, M.T. et al., 2008. Comparative study of pulmonary responses to nano-and submicron-sized ferric oxide in rats. ***Toxicology***, 247(2), pp.102-111.